REVIEW   **Open Access**

CrossMark

A survey on modeling interference and blockage in urban heterogeneous cellular networks

Martin Taranetz[*] and Martin Klaus Müller

Abstract

In this paper, we provide a survey on abstraction models for evaluating aggregate interference statistics in urban heterogeneous cellular networks. The two principal interference shaping factors are the path loss attenuation and the interference geometry. For both factors, our survey systematically summarizes state-of-the-art models and outlines their strengths and weaknesses. In the context of path loss attenuation, we give an overview on the basic propagation mechanisms and the various approaches for their abstraction. We specifically elaborate on random shape theory and its application for representing blockages in indoor and outdoor scenarios. In terms of interference geometry, we present techniques from stochastic geometry as well as deterministic approaches, outlining their evolution and limitations. Throughout the paper, challenges under discussion are scenarios with both indoor and outdoor environments, distance-dependent shadowing due to blockages, and correlations among node and blockage locations as well as the distinction between cell center and cell edge. Our goal is to raise awareness on not only the validity and tractability but also the limitations of state-of-the-art techniques. The presented models were chosen with regard to their adaptability for a broad range of scenarios. They are therefore expected to be adopted for describing the fifth generation of mobile networks (5G).

Keywords: Interference modeling, Aggregate interference, Blockage, Fading, Path loss, Shadowing, Stochastic geometry, Random shape theory, Point process, Urban, Heterogeneous networks, 5G

1 Review

Massive network densification and heterogeneity are two major trends heralding the fifth generation of mobile cellular networks (5). Heterogeneous networks are commonly identified as systems comprising multiple types of base stations (BS) that are distinguished by their transmit power and backhaul and radio access technology as well as the experienced propagation conditions. In such topologies, the aggregate co-channel interference from other cells (also referred to as *other-cell interference, external interference, network interference*, or simply *interference*) is one of the main performance limiting factors [1–7]. At the same time, it forms the basis for determining the signal-to-interference ratio (SIR) and the other-cell interference factor (OCIF), which constitute fundamental metrics for assessing the performance of mobile networks.

The SIR commonly refers to the ratio between the desired signal power and the total interference power [1, 3]. In contrast, the OCIF (also termed *f-factor* or *interference factor*) is traditionally defined as the ratio of the other-cell interference to the *own-cell interference* (also denoted as *same-cell* or *inner-cell interference*) [8–11]. Own-cell interference arises, e.g., as *multiple access interference* due to cross correlation of spread-spectrum signals in a code-division multiple access (CDMA) system [8]. In more recent work, the OCIF is defined as the ratio of the other-cell received power to the total inner-cell received power, encompassing both the desired signal as well as the own-cell interference [5–7, 12, 13]. This definition is still valid for mobile systems without own-cell interference, such as orthogonal frequency-division multiple access (OFDMA) [6, 14]. Therefore, the thorough statistical description of aggregate co-channel interference from other cells is essential for system analysis and design. The main goal of the interference analysis is to *capture key*

*Correspondence: mtaranet@nt.tuwien.ac.at
Christian Doppler Laboratory for Dependable Wireless Connectivity for the Society in Motion, Technische Universität Wien, Vienna, Austria

characteristics of the interference as a function of *relatively few parameters*. Although abstractions such as the Wyner model and the hexagonal grid first appeared two or even five decades ago [15, 16], mathematically tractable interference statistics are still the exception rather than the rule.

A frequently applied approach is the *Gaussian random process* [17, 18]. The model is reasonably accurate when aggregating a large number of interferers without a dominant term such that the central limit theorem (CLT) applies [19, 20]. In many cases, the probability density functions (PDFs) will exhibit heavier tails than those anticipated by the Gaussian approach [1, 21–25].

In general, the PDF is unknown, and aggregate interference is typically characterized by either the Laplace transform (LT), the characteristic function (CF), or the mobility generating functional (MGF), respectively [26]. In this article, the LT is considered most relevant due to its suitability for random variables (RV) with non-negative support and its *moment-generating properties*. Moreover, the CF and the MGF can directly be deduced from the LT by basic identities. Let I denote a RV with PDF $f_I(x)$, representing the aggregate interference. Then, its LT is given as

$$\mathcal{L}_I(s) = \mathbb{E}\left[e^{-sI}\right] = \int_0^\infty f_I(x)e^{-sx}dx. \tag{1}$$

The nth moment of I is determined by

$$\mathbb{E}\left[I^n\right] = (-1)^n \left.\mathcal{L}_I^{(n)}(s)\right|_{s=0}, \tag{2}$$

where $\mathcal{L}_I^{(n)}(s)$ refers to the nth derivative of $\mathcal{L}_I(s)$. In theory, a statistical distribution is fully characterized by specifying all of its moments, given that all moments exist and the MGF converges. Practical approaches in wireless communication engineering usually exploit only the first few of them. Application examples include *moment matching* and *deriving performance bounds by inequalities* such as the Markov inequality [27].

The two main interference shaping factors are the *path loss attenuation* and the *interference geometry* [1, 14, 28–34]. The path loss attenuation describes the difference between the transmit and receive power levels. The interference geometry condenses the transmitter locations and the channel access scheme [14, 35, 36].

1.1 Our contributions

This article provides a survey on state-of-the-art modeling and abstraction of these two factors. We particularly focus on urban environments, as they form the major field of application for heterogeneous mobile networks. In the context of signal propagation modeling, we elaborate on the basic propagation mechanisms as well as their abstraction. The main novelty of this section lies in a survey on

models based on random shape theory. Those are applied for investigating the impact of blockages in indoor and outdoor scenarios. In the context of interference geometry, we outline models for abstracting the BS locations. In comparison to related surveys, we discuss both stochastic *and* deterministic models. We address strengths and limitations, and demonstrate their application by means of a case study.

This paper exclusively addresses *aggregate co-channel interference from other cells*. Other types of interference encompass *inter-carrier, inter-symbol, inter-layer, inter-user*, and *own-cell* interferences. Each of these interference types has its particular characteristics and, thus, requires its own mathematical framework. Due to space limitations, these kinds of interferences are considered beyond the scope of this paper.

The majority of aggregate interference models aims at describing downlink transmissions. For this reason, we employ the terms *BS* and *receiver*, when exclusively referring to the downlink, and *transmitter* and *receiver*, when pointing out that a model is equivalently applicable for up- and downlink. In this article, the term *tier* either refers to a ring of transmitters in a grid-based setup or the specific part of a heterogeneous network, which is associated with a certain class of transmitters, such as macro-BS and small cell BSs, respectively. The particular meaning becomes apparent from the context. Since the focus of this paper is placed upon cellular networks, we consider the field of device-to-device (D2D) communications beyond the scope of this paper.Throughout the paper, we comment on the adaptability of the presented models for abstracting (5G) topologies.

1.2 Related work

The closest related works to the contribution in this paper are [37] in the context of signal propagation modeling and [26] in the domain of interference geometry abstraction.

The authors of [37] provide a broad overview on large-scale path loss modeling. They specifically elaborate on seven different types of path loss models, presenting their advantages and drawbacks. In this paper, we briefly summarize these *traditional approaches*. Compared to [37], our focus is rather placed upon heterogeneous networks in urban environments. We specifically address the abstraction of large object blockage by means of random object processes.

The authors in [26] provide a survey on stochastic geometry models for single-tier and multi-tier cognitive mobile networks. They summarize the five most prominent techniques to utilize the LT of the aggregate interference for modeling the network performance. In this paper, we briefly outline these techniques in Section 3.1.2. While the authors of [26] mainly focus on the opportunities of

the stochastic geometry analysis, in this paper, we also address its limitations. Moreover, we discuss deterministic models, which, to the best of our knowledge, have not yet been surveyed.

1.3 Organization

This paper is organized as follows. In Section 2, we scrutinize signal propagation mechanisms. We review traditional models and place particular focus on statistical models for representing blockages. In Section 3, we investigate the abstraction of transmitter locations and the impact of channel access mechanisms. We elaborate on techniques from stochastic geometry and their major insights.

We also shed light on the evolution of deterministic models. We address the limitation of both approaches and compare them by means of a case study. Section 4 outlines further aspects of interference modeling. Section 5 concludes the work.

2 Signal propagation modeling

Due to the broadcast nature of the wireless medium, any signal sent from a transmitter experiences various kinds of distortion along its way to the receiver. These will depend on the environment as well as the location of the transmitter and the receiver. In this section, we discuss techniques for abstracting the mechanisms that govern the signal propagation. An overview is provided in Fig. 1.
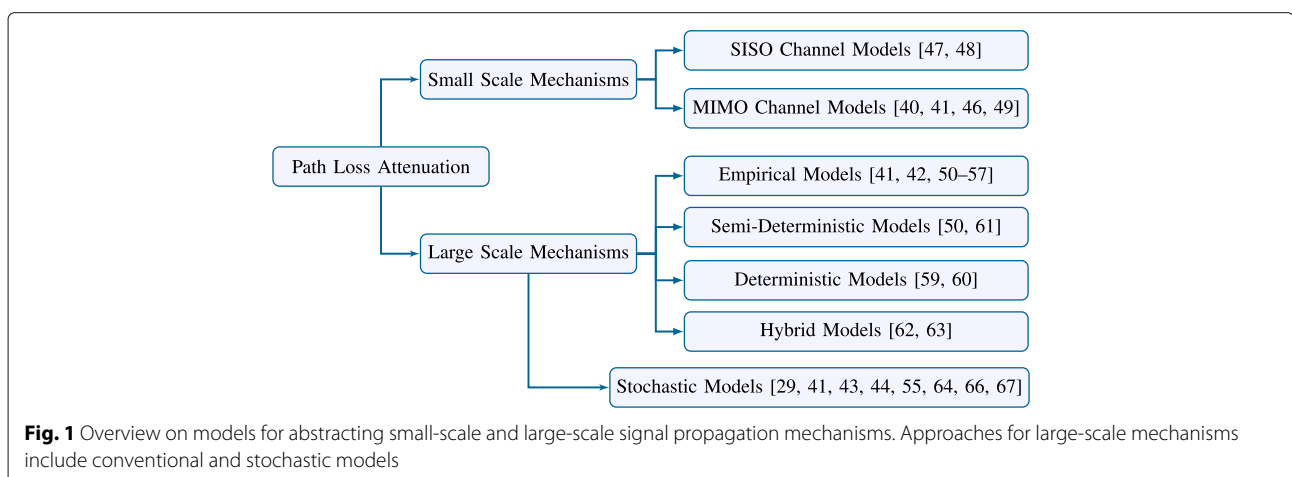
2.1 Signal propagation mechanisms

Signal propagation is governed by four basic mechanisms [38]: *free-space loss* (distance-dependent loss along a line of sight (LOS) link), *reflections* (waves are reflected by objects that are substantially larger than the wavelength), *diffractions* (based on Huygen's principle, secondary waves form behind large impenetrable blockages), and *scattering* (energy is dispersed in various directions by objects that are small relative to the wavelength). These effects individually perturb the signal traveling from a transmitter to a receiver, thus determining the instantaneous signal strength. A formal definition of the path loss attenuation in decibel is given as

$$PL = P_t - P_r + G_t + G_r, \tag{3}$$

where P_t and P_r represent the transmit and receive power levels and G_t and G_r refer to the transmit and receive antenna gains. When sectorized scenarios are considered, the antenna characteristics can be incorporated in G_t, including the antenna orientation and the angular dependent antenna gains, respectively. The losses caused by the four basic propagation mechanisms constitute the difference between P_t and P_r. In principle, each mechanism is well known and the resulting path loss attenuation can be exactly determined by evaluating Maxwell's equations. Such calculation requires a very accurate description of the environment. In practice, it is infeasible to solve for a single point to point link, let alone the evaluation of an entire network. Real-world propagation environments exhibit a complex structure, which leads to the necessity of abstraction. The requirement for a path loss attenuation model is to be simple enough to assure tractability while still capturing the most prominent effects of a realistic scenario.

In comparison to analytical studies, simulations enable a low degree of abstraction, i.e., they allow to incorporate a large amount of details. Path loss attenuation models may even follow a certain generation procedure, such as in the 3rd Generation Partnership Project (3GPP) spatial channel model (SCM) [39], the Wireless World Initiative New Radio (WINNER) model [40], and the 3GPP three-dimensional (3D) channel model [41]. In these models, the environment is represented by statistical parameters and the exact propagation conditions are computed at

Fig. 1 Overview on models for abstracting small-scale and large-scale signal propagation mechanisms. Approaches for large-scale mechanisms include conventional and stochastic models

runtime. Such models are infeasible for analytical considerations, where signal propagation is commonly described by deterministic laws and RVs, as presented in the next section.

The basic propagation mechanisms are affecting the transmission in both the *below 6-GHz domain* as well as the *millimeter wave (mmWave) domain*. Therefore, most of the models that are described in the following can be adapted to represent either domain, by adjusting the influence of the individual effects accordingly. Several 5G specific references were added, in order to capture the ongoing work in this direction [42–45].

2.2 General modeling approach

A common approach for modeling path loss attenuation is expressed as

$$\mathrm{PL} = \underbrace{L(d,f) + X_\sigma}_{\text{large-scale path loss}} + \underbrace{F}_{\text{small-scale path loss}}, \qquad (4)$$

where $L(d,f)$ refers to the mean path loss, X_σ is the shadowing, and F denotes the small-scale fading. The term $L(d,f)$ is mainly based on the effect of free-space path loss, which depends on the distance d between a transmitter and a receiver as well as the carrier frequency f. Note that it is independent of the node locations within the scenario. The RV X_σ corresponds to the shadowing caused by blockages. The RV F primarily captures the effects of the multi-path propagation. It is important to note that (4) does not model each of the four basic propagation mechanism, as presented in Section 2.1, separately. Each of the three terms rather incorporates *all* mechanisms to a certain extent.

The terms in (4) can be grouped into *large-scale path loss*, including the mean path loss and the shadowing, and *small-scale path loss* referring to F. This terminology is derived from the scale in space and time, where severe variations are expected to occur. The *small-scale component* can show large fluctuations in a short period of time as well as within few wavelengths. The corresponding models are commonly denoted as *channel models* [40, 41, 46–48]. They incorporate the effects of single-input single-output (SISO) and multiple input multiple output (MIMO) transmissions and may include correlations over time and frequency. Modeling the influence of these effects is of interest when instantaneous transmission characteristics are investigated. In the following, we focus on the long-term average trends of the path loss, referring to the *large-scale* component in (4). A survey on MIMO channel models is provided in [49] and is considered beyond the scope of the paper.

2.3 Traditional path loss attenuation models

In literature, a substantial number of large-scale path loss models have been reported. They can be categorized into four groups: *empirical models*, *deterministic models*, *semi-deterministic models*, and *hybrid models*. The main distinctive characteristic of these models is the trade-off between accuracy and complexity. While these models aim at representing the large-scale component in (4), they do not necessarily distinguish mean path loss and shadowing.

2.3.1 Empirical models

Empirical models are typically obtained from measurement campaigns in a certain environment and describe the characteristics of the signal propagation by a deterministic law or some RV. They can be characterized by only few parameters and have found wide acceptance for analytical studies and simulations.

Examples for *empirical* path loss laws include the *COST 231 One Slope Model* and the *COST 231 Hata Model* [50]. The most famous example for a *random* abstraction of large-scale path loss is *log-normal shadowing*, where the effect of blockages is crammed into a log-normally distributed RV. The variance of the distribution depends on the environment and has to be determined by measurements. Thus, the model is only valid for specific scenario and requires and empirical calibration step. In real-world scenarios, the locations of large objects will be highly correlated [51]. Interference correlation in scenarios with stochastic node locations (conf. Section 3.1) is scrutinized in [52, 53]. The correlation in these papers is almost exclusively obtained by the static locations of the nodes, whereas the correlation of collocated blockages is not taken into account [54]. The authors of [54] present a correlated shadowing model by exploiting a Manhattan Poisson line process. They provide a promising method to better understand the generative processes that govern the shadowing. On the other hand, the usefulness of their approach is limited to Manhattan-type urban geometries.

Recent studies on blockage effects in urban environments indicate the dependency of shadowing on the link length [54, 55]. It follows the intuition that a longer link increases the likelihood of buildings to intersect with it. Such propagation characteristics have also been discussed recently within the 3GPP [41, 56] and cannot be reproduced by the log-normal model. As presented in Section 2.4, they can be reflected by approaches based on random shape theory.

The authors in [57] propose a multi-slope model, where the path loss law itself is a piecewise function of the distance. A related approach is to distinguish between LOS and non-line of sight (NLOS) conditions and to adapt the path loss model accordingly. In this case, it is crucial to decide whether a given link is in LOS or NLOS,

depending on the link length [42]. A combination of the multi-slope model and the distinction between LOS and NLOS conditions is reported in [58].

2.3.2 Deterministic models

The goal of deterministic models is to represent the characteristics of a specific scenario with high accuracy and to include all basic propagation mechanisms. Consequently, deterministic models are characterized by the need for detailed site-specific information and large computation efforts. Two classes of deterministic models have been reported in literature. *Finite-difference time-domain models* try to replace Maxwell's differential equations with finite-difference equations, thus exhibiting a certain degree of abstraction. *Geometry models* rely on geometric rays that interact with the specified objects and are also referred to as *ray-tracing models* [59, 60]. Due to the fundamental dependency on site-specific information, it is difficult to draw general conclusions from the attained results.

2.3.3 Semi-deterministic models

Empirical and deterministic models form the two opposing ends of the accuracy-complexity trade-off. Combining both approaches leads to *semi-empirical* and *semi-deterministic* models. These models still incorporate some site-specific information while parameterizing other parts of the model by results from measurement campaigns. Some effects such as reflections may be ignored to reduce the complexity of the model. A frequently applied representative of semi-empirical models is the COST 231 Walsch-Ikegami Model [50]. A more recent, map-based approach has been proposed in [61] within the scope of the METIS 2020 project. It follows the concept that building heights are extracted from map data and are then used to estimate the path loss.

2.3.4 Hybrid models

Hybrid models combine multiple of the previously discussed propagation models. This is especially beneficial when scenarios contain sections with fundamentally different propagation conditions. A classic example is outdoor-to-indoor communication [62, 63], where the output of a 3D semi-deterministic geometry model is transformed into a 2D geometry model for describing the indoor propagation.

2.4 Stochastic blockage models

In this section, we focus on a newly emerging class of path loss models that describes attenuations due to blockages by statistical parameters. These models can expediently be used for indoor and outdoor scenarios, are mathematical tractable, and can be characterized by few parameters. Their formulation is based on concepts from *random shape theory*, which represents the formal framework around random objects in space [64].

While we focus on large-scale blockages such as walls and buildings, the authors of [45] show that the obstruction due to the human body can be modeled in a similar way. Body blockage is particularly distinct in the mmWave domain, where even the attenuation due to foliage affects the signal propagation, as investigated, e.g., in [65].

Let $\mathcal{O}$ denote a set of objects on $\mathbb{R}^n$, which are closed and bounded, i.e., have finite area and perimeter. For instance, $\mathcal{O}$ could be a collection of lines, circles, or rectangles on $\mathbb{R}^2$ (conf. Fig. 2) or a combination of cubes in $\mathbb{R}^3$. For each object in $\mathcal{O}$, a *center point* is determined, which has to be well-defined but does not necessarily relate to the object's center of gravity. Non-symmetric objects additionally require to specify the orientation in space by a directional unit vector. In the analysis of mobile cellular networks, the objects in $\mathcal{O}$ represent blockages such as buildings and walls.

A *random object process (ROP)* is constructed by randomly sampling objects from $\mathcal{O}$ and placing their corresponding center points at the points of some point process (PP). The orientation of each object is independently determined according to some probability distribution.

In general, a ROP is difficult to analyze, particularly when there are correlations between sampling, location, and orientation of the objects. For the sake of tractability, a *Boolean scheme* is commonly applied in literature [29, 43, 44, 55, 66, 67]. It satisfies the following properties: (i) the center points form a Poisson point process
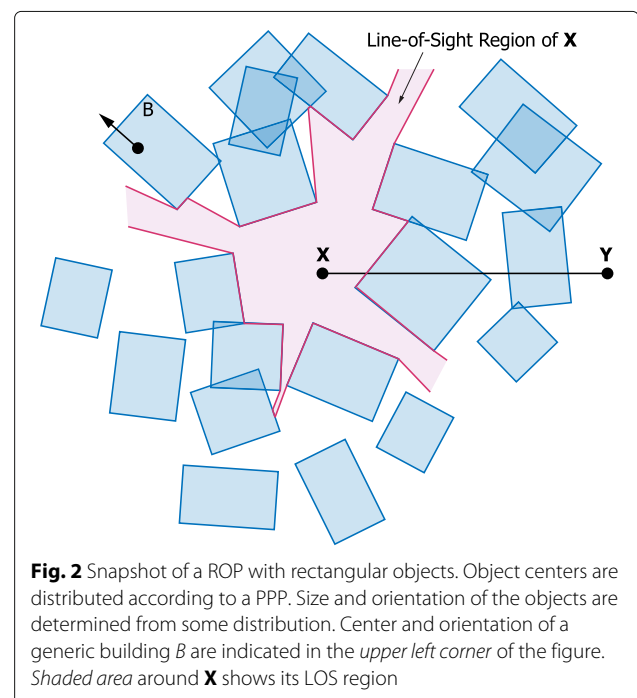

Fig. 2 Snapshot of a ROP with rectangular objects. Object centers are distributed according to a PPP. Size and orientation of the objects are determined from some distribution. Center and orientation of a generic building *B* are indicated in the *upper left corner* of the figure. *Shaded area* around **X** shows its LOS region

(PPP); (ii) the attributes of the objects such as orientation, shape, and size are mutually independent; and (iii) for each object, sampling, location, and orientation are also independent. These assumptions of independence enable the tractability of the analysis. On the other hand, they omit correlations among blockages, as observed in practical scenarios.

Let **X** and **Y** denote the locations of the receiver and the transmitter, as indicated in Fig. 2. Further, let **XY** refer to the path between the two nodes. In a Boolean scheme, the number K of blockages crossing a link **XY** is a *Poisson RV* with mean

$$\mathbb{E}[K] = \lambda_B \mathbb{E}[V(\mathbf{XY} \oplus B)], \qquad (5)$$

where λ_B denotes the density of the blockage centers and $B \in \mathcal{O}$ [55]. The operator $\oplus$ refers to the *Minkowski sum*, which is defined as $\mathcal{A} \oplus \mathcal{B} = \bigcup_{\mathbf{x}\in\mathcal{A}, \mathbf{y}\in\mathcal{B}}(\mathbf{x}+\mathbf{y})$ for two compact sets $\mathcal{A}$ and $\mathcal{B}$ in $\mathbb{R}^n$, and $V(\cdot)$ is its *volume*. The expectation in Eq. 5 is calculated with respect to the objects in $\mathcal{O}$ thus yielding the Minkowski sum with the *typical building*.

First note that $\mathbb{E}[K]$ will depend on the *length* $|\mathbf{XY}|$ of the link. Another direct consequence of the model is the probability that no blockage obstructs the link **XY**, also referred to as *LOS probability*. It is obtained by applying the void probability of a Poisson RV: $\mathbb{P}[K = 0] = \exp(-\lambda_B \mathbb{E}[V(\mathbf{XY} \oplus B)])$. Notably, the exponential decay has been confirmed by measurement campaigns and has also been incorporated into the 3GPP standard [41].

Let γ_k denote the ratio of power loss due to the kth blockage. Then, the *power loss* caused by the blockages in a Boolean scheme is given by $\Gamma = \prod_{k=1}^{K} \gamma_k$, where K refers to the random number of blockages [55]. Assuming that γ_k are independent and identically distributed (i.i.d.) RVs on $[0,1]$ and K is a Poisson RV with means as given in Eq. 5, the distribution of Γ is in general not accessible in closed form. Recent approaches in literature therefore resort to the moments of Γ [55, 67]. The nth moment of Γ is obtained as $\mathbb{E}[\Gamma^n] = \exp(-\lambda_B \mathbb{E}[V(B)])(1 - \mathbb{E}[\gamma_k^n])$. Hence, on average, blockages impose an additional exponential attenuation on the mean path loss (conf. (4)). It is important to note that in this approach, reflections are ignored. They can implicitly be incorporated

by distinguishing between LOS and NLOS conditions (cf. Section 2.3.1) and adapting the path loss exponent accordingly [68].

To provide more intuition on this general result, we present an application example along the lines of [66]. In an indoor scenario, blockages are mainly constituted by walls. We represent these walls by a ROP of lines with random length and orientation. Then, the process is defined by the triple $\{X_i, L_i, \Theta_i\}$, where X_i corresponding to the PPP of wall-center positions with density λ_W, L_i is the wall length, which is distributed according to some distribution $f_L(n)$, and Θ_i denotes the wall-orientation, which is uniformly distributed in $[0, 2\pi]$. According to the introduced framework, the number K of walls blocking a link **XY** is a Poisson RV with mean

$$\mathbb{E}[K] = \frac{2\lambda_W \mathbb{E}(L)\,|\mathbf{XY}|}{\pi}. \qquad (6)$$

On the one hand, this result exhibits the dependency of $\mathbb{E}[K]$ on the link length $|\mathbf{XY}|$. On the other hand, it shows that the characteristics of a realistic environment can straightforwardly be incorporated into the model, by adapting the parameter λ_W as well as the distribution of W_i and Θ_i, respectively. This information can straightforwardly be extracted from real map data. When using convex two-dimensional (2D) objects instead of lines, the ROP is well suited to represent urban environments [55, 67].

A comparison of the discussed models is provided in Table 1. It includes necessary prior knowledge on the environment, mathematical tractability, flexibility, and accuracy. The next section elaborates on models for abstracting the interference geometry.

3 Interference geometry

When designing a mobile cellular system, its main aspects should hold across a wide range of deployment scenarios. Transmitter locations are commonly abstracted to some baseline model. For more than three decades, its most famous representative, the hexagonal grid model, has successfully withstood the test of time [16]. It has extensively been employed in both academia and industry and has found wide acceptance as a reasonably useful model

Table 1 Comparison of discussed signal propagation models

	Prior environment knowledge necessary	Mathematical tractability	Flexibility	Accuracy
Empirical models	Low	✓	Low	Low
Semi-deterministic models	Medium	✓	Medium	Medium
Deterministic models	High	✗	Low	High
Hybrid models	Variable	✗	Variable	Variable
Stochastic models	Medium	✓	High	Medium

to represent well-planned *homogeneous* BS topologies [69–72].

In the context of heterogeneous networks, small cell locations are oftentimes beyond the scope of network planning and hence exhibit a more random nature [3, 73–77]. Without preliminary information, the best statistical assumption is a uniform distribution over space, corresponding to complete spatial randomness [78]. In this case, transmitter locations can conveniently be described by some PP that further allows to leverage techniques from *stochastic geometry*. This powerful mathematical framework has gained momentum in recent years as the only available tool that provides a rigorous approach for modeling, design and analysis of a multi-tier network topologies [1, 4, 28–30, 33, 35, 55, 72, 79–85]. It is also considered an important approach for scrutinizing ultra dense networks (UDNs) in 5G topologies (see, e.g., [57, 58]).

Spatial randomness constitutes the philosophical opposite of a regular structure. As a results, these two extreme cases yield lower and upper performance bounds for any conceivable heterogeneous network deployment [76].
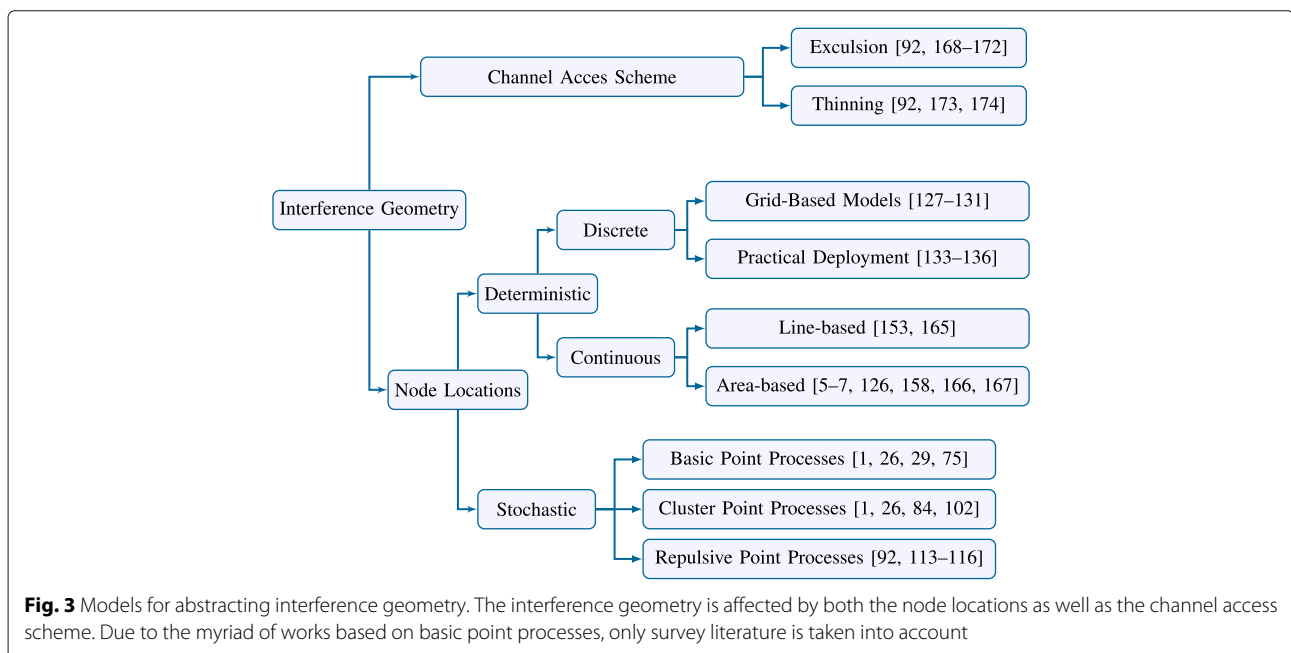
The first part of this section elaborates on the lower performance boundary, providing an overview on techniques from stochastic geometry. The second part addresses the upper bound, focusing on regular models and viewing them in the broader context of deterministic structures. In the third part of the section, a comparison in the form of a case study is carried out. In the forth part, the impact of channel access mechanisms is discussed. An overview on interference geometry models is provided in Fig. 3.

3.1 Stochastic models

The roots of stochastic geometry date back to shot noise studies of Campbell in 1909 [86, 87] and Shottky in 1918 [88]. In a planar network of nodes, which are distributed according to some PP, interference can be modeled by a generalized shot noise process [89, 90]. Key metrics such as coverage and rate had not been determined at this time. The idea of applying this framework for cellular networks appeared in the late 1990s [4, 80, 81]. Comprehensive surveys on literature related to stochastic geometry are already available, e.g., in [26, 75, 84]. For this reason, this section shall be confined to a selection of significant insights and shall outline limitations of this framework, which have found much less attention in literature.

3.1.1 Analysis of stochastic geometry

The analysis of stochastic geometry is based upon the concept of abstracting BS locations to some PP. As a result, it yields *spatial averages* over a substantial number of network realizations. When the nodes of a homogeneous BS deployment are distributed according to a PPP, i.e., they are assumed to be uniformly scattered over the infinite plane, and the fading is represented by i.i.d. non-negative RVs, the PDF of the aggregate interference yields a *skewed stable* distribution [1, 30, 91]. Yet, this is the only available case in literature that leads to known interference statistics. Still, except for a Lévy distribution, which is obtained by assuming a path loss exponent of 4, it does not result in any closed-form expressions for the aggregate interference PDF [26].

Fig. 3 Models for abstracting interference geometry. The interference geometry is affected by both the node locations as well as the channel access scheme. Due to the myriad of works based on basic point processes, only survey literature is taken into account

The success of stochastic geometry is rather rooted in the fact that it provides a means for systematically evaluating the Laplace transform of the aggregate interference, as defined in Eq. 1. The enabling identity is the probability generating function (PGFL): Let Φ denote an arbitrary PP. Then, its PGFL formulates as

$$\mathcal{G}[g] = \mathbb{E} \prod_{\times \in \Phi} g(\times), \qquad (7)$$

where $g(x) : \mathbb{R}^d \to [\, 0, \infty)$ is measurable.

It proves particularly useful to evaluate the LT of the sum $\sum_{\times \in \Phi} f(\times)$:

$$\mathbb{E}\left[\exp\left(-s \sum_{\times \in \Phi} f(\times)\right) \right] = \mathbb{E}\left[\prod_{\times \in \Phi} \exp(-sf(\times)) \right]$$
$$= \mathcal{G}[\exp(-sf(\cdot))], \qquad (8)$$

which characteristically appears in the analysis of aggregate interference with *discrete* node location models (continuous models will be explained in Section 3.2). The function $f(\cdot)$ represents the received power from an individual interferer at location $\times$. Consequently, $I = \sum_{\times \in \Phi} f(\times)$. Since I is a RV that is strictly positive, its LT always exists. It is important to note that the exact expressions for the LT, MGF, and CF are only available for *basic PPs*, encompassing PPP, binomial point process (BPP), and Poisson cluster process (PCP). For other types of PPs such as hardcore processes, only *approximations* are available.

3.1.2 Performance evaluation

Due to the *non-existence* of the aggregate interference PDF, it is generally not possible to derive exact performance metrics such as outage probability, transmission capacity, and average achievable rate. The authors in [26] summarize five techniques to go beyond moments and to model the network performance:

- #1: Resort to Rayleigh fading on desired link [3, 92–102]
- #2: Resort to dominant interferers by region bounds or nearest n interferers [85, 103]
- #3: Resort to Plancherel-Parseval theorem [104]
- #4: Directly invert the LT, CF, or MGF [22, 30, 91, 105–107]
- #5: Approximate interference by known PDF [63]

Using technique #1, the highly cited paper of Andrews et al. outlines three fundamental insights from the analysis of stochastic geometry [3]:

- In comparison to an actual BS deployment, models from stochastic geometry provide accurate lower bounds on the performance, while grid-based models yield upper bounds.

- With certain assumptions regarding path loss and fading, simple expressions for the coverage probability and the mean transmission rate can be derived.
- When the network is interference limited, i.e., the noise is considered negligible w.r.t. to the interference, the SIR statistics are independent of the BS density. Intuitively, the increasing aggregate interference is perfectly compensated by the lower average distance to the desired node.

The authors of [108] extended these results to heterogeneous cellular networks with an arbitrary number of tiers. Despite all the benefits of the stochastic approach, there are certain shortcomings one should be aware of when applying this framework. In the following, we provide a list with no claim to completeness.
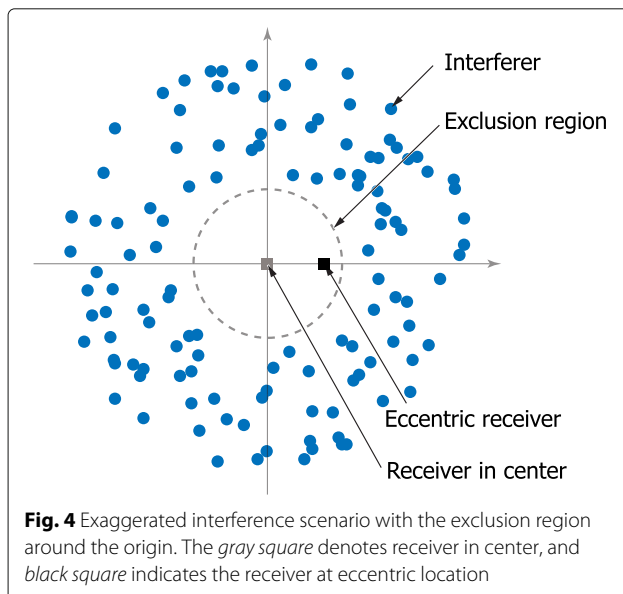
3.1.3 Limitations

[**Spatial averages**] The analysis of stochastic geometry is based on *averaging* over an ensemble of spatial realizations. When the point process is ergodic, this is equivalent to averaging over a substantial number of spatial locations. Performance metrics vary from one interferer snapshot (i.e., realization of a point process) to another. Hence, the averaging only provides *first-order* statistics and is thus argued to hide the effect of design parameters on the uncertainties due to such variations [26]. To extend the analysis of stochastic geometry beyond spatial averages, the authors in [109] identify three sources of variability: (i) the variable distance between a node and its associated user; (ii) the variable transmission probability, which is particularly prominent in networks with contending nodes (e.g., Wireless Fidelity (Wi-Fi) and carrier sense multiple access (CSMA)); and (iii) the variability in the likelihood of successful reception. In [110] and [109], the full statistics of the SIR, also denoted as *meta distribution* of the SIR, and the throughput distribution are *approximated*.

[**Spatial correlations**] A major disadvantage of stochastic models is the difficulty to model correlations among node locations [71, 111, 112]. Those appear when reflecting topological and geographical constraints or accounting for the impact of network planning, which is not expected to loose relevance for the macro-tier in 5G networks. Therefore, it is considered imperative to investigate system models with a certain degree of regularity. In fact, the simplest and *most commonly used* PP, the PPP, assumes *completely uncorrelated* node locations. In the context of stochastic geometry, regularity can to some extent be reflected by *repulsive PPs*. Such processes impose a certain minimum acceptable distance between two BSs. When the exclusion region is fixed, the process

is termed *hardcore PP*. When it is defined by a probability distribution, the process is denoted as *softcore PP*. Hard- and softcore processes significantly complicate the interference analysis due to the non-existence of the PGFL. Therefore, they require to approximate the LT of the aggregate interference or the PDF itself. Besides that, the most promising representative, the Matérn hardcore point process (HCPP), contains flaws that still have to be addressed [113–116]. It underestimates the intensity of points that can coexist for a given hardcore parameter.

[**Measuring heterogeneity**] Given a realistic node distribution, a particular challenge is to find a PP with the same structural properties. An objective measure for the *degree of heterogeneity*, also known as *degree of clustering* or *clumping factor*, should be independent of the number of nodes and the size of the area, in which the nodes are distributed as well as linear operations such as rotating and shifting [117]. Classical statistics include the J-function, the L-function [84], and Ripley's K-function [118–120]. While the J- and the L-functions are related to inter-point distances, Ripley's K-function measures second-order point location statistics. Both metrics do not allow to *unambiguously* identify different PPs. In [72], the authors propose to apply the coverage probability as a goodness of fit measure. Again, this measure does not allow to discriminate different models.

[**Asymmetric impact of interference**] Another factor that stalls the analysis of stochastic geometry is the incorporation of an asymmetric impact of the interference, as indicated by the exaggerated interference scenario in Fig. 4. With few exceptions, convenient expressions

Fig. 4 Exaggerated interference scenario with the exclusion region around the origin. The *gray square* denotes receiver in center, and *black square* indicates the receiver at eccentric location

are only achieved by assuming spatial *stationarity* and *isotropy* of the scenario, i.e., a receiver being located in the center. In [121, 122], the authors employ a *fixed cell* approach for scrutinizing eccentric receiver locations. Their method is shown to achieve accurate results only in combination with an approximation of the interference statistics by a Gamma distribution. Otherwise, notions such as *cell-center* and *cell-edge* are generally not accessible in the analysis.
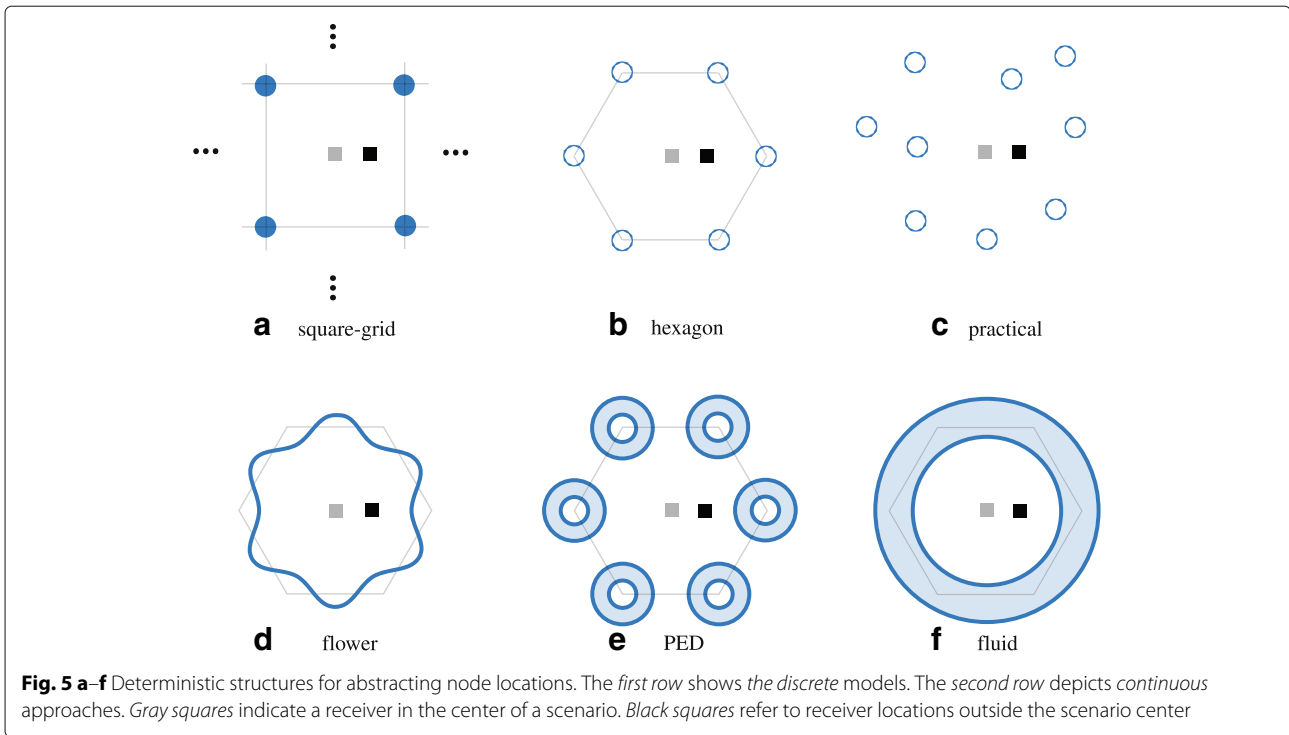
3.2 Deterministic structures
The broad acceptance of models based on stochastic geometry has diverted attention away from the still ongoing improvement of deterministic structures, with their most famous representative being the hexagonal grid model. They allow to reflect the impact of the network planning, which might increasingly disappear with the emergence of self-organizing networks (SON) [123–125], and also account for more fundamental limitations such as topological and geographical constraints. In this section, we review efforts to facilitate the interference analysis using these structures, even allowing to represent multi-tier heterogeneous topologies.

Deterministic structures can broadly be categorized into *discrete* and *continuous* models [126]. Discrete models are characterized by modeling each node individually. The amount of nodes can either be finite or infinite and the arrangement of nodes follows a certain structure such as a circle or a grid, as illustrated in Fig. 5. Continuous models assume the contributions from the interferers to be uniformly distributed over a certain *n*-dimensional geometric shape, such as a circle or a ring.

3.2.1 Discrete models
Interference analysis in discrete models is based on evaluating the impact of each individual interferer on the receiver and then aggregate them. The node locations are commonly modeled along a finite or infinite regular structure, such as a square grid (also referred to as *Manhattan-type model* [127–131]) or a hexagon (see. e.g., [63, 132]), as depicted in Fig. 5. It should be noted that realistic scenarios, which utilize data from network operators, such as in [133–136], also belong to this class of models. Such data may also include information about the boresight directions of the sector antennas, which is required for the calculation of the path loss (conf. Section 2.1), as well as the antenna tilting.

As explained in Section 2.1, signal propagation is usually characterized by some deterministic law and a random component accounting for the fading. Consequently, in a discrete regular structure, the aggregate interference can be viewed as a finite or infinite *sum of weighted RVs* with the weights being straightforwardly obtained from geometric considerations.

Fig. 5 a–f Deterministic structures for abstracting node locations. The *first row* shows *the discrete* models. The *second row* depicts *continuous* approaches. *Gray squares* indicate a receiver in the center of a scenario. *Black squares* refer to receiver locations outside the scenario center

Certain fading distributions, such as Rayleigh, log-normal, or Gamma, enable to exploit a myriad of literature on the sum of weighted RVs [47, 48, 137–152]. The majority of these reports make use of variants of the CF or the MGF. When the receiver is located in the center of a symmetric grid, as indicated by the gray squares in Fig. 5, the weights are all equal or can be summarized into groups. As a result, this scenario often leads to closed-form expressions for the distribution of the aggregate interference, as demonstrated, e.g., in [153]. In the general case, when the receiver is located outside the scenario center (conf. Figs. 4 and 5), the weights are all different and the performance analysis is stalled with an inconvenient sum of RVs. To overcome this issue, two approaches are commonly applied in literature:

- Scrutinize individual link statistics to gain understanding on overall interference behavior [13, 154, 155]. The focus of these models mainly lies on link-distance statistics. While they do not lead to convenient expressions for the moments and the distribution of the aggregate interference, they allow to evaluate arbitrary receiver locations in a cell.
- Approximate aggregate interference distribution by known distribution [6, 9, 13, 14, 27, 32, 156–158]. It is well-studied that the CLT and the corresponding Gaussian model provide a very poor approximation for modeling aggregate interference statistics in large

wireless cellular networks [30, 159, 160]. Its convergence can be measured by the Berry-Esseen inequality [161] and is typically thwarted by a few strong interferers. The resulting PDF exhibits a heavier tail than what is anticipated by the Gaussian model [30]. Resorting to the approximation of the aggregate interference distribution by a known parametric distribution imposes two challenges: (i) the choice of the distribution itself and (ii) the parametrization of the selected distribution. Although there is *no known criterion* for choosing the optimal PDF, its tractability for further performance metrics as well as the characteristics of the spatial model, the path loss law, and the fading statistics advertise certain candidate distributions [32].

A class of continuous probability distributions that allow for positive skewness and non-negative support are normal variance-mean mixtures, in particular the normal inverse Gaussian distribution. The main penalty of such generalized distributions is the need to determine up to four parameters, which typically exhibit non-linear mappings when applying moment or cumulant matching [32]. Hence, it is beneficial to resort to special cases with only two parameters. Inverse Gamma, inverse Gaussian, log-normal, and Gamma distribution have frequently been reported to provide an accurate abstraction of the aggregate interference statistics, e.g., in [32, 160, 162], [32, 160], [151], and [32, 121, 163, 164], respectively.

It is expected that discrete models will play an important role in 5G topologies for representing the *regular* part of the network [152, 153].

3.2.2 From discrete to continuous

The discrete models discussed in the previous paragraph aim at reproducing the actual site locations. The authors in [152] propose to represent arbitrary BS topologies by nodes along circles, where the nodes do not necessarily represent physical sources. They rather correspond to mapping points of an angle-dependent power profile, as illustrated in Fig. 6. The authors provide a mapping scheme that enables to accurately preserve the interference statistics of *fully random, heterogeneous topologies* with 10,000 and more BSs by some ten nodes. It corroborates the intuition that the number of principal interferers is typically low and therefore allows to substantially reduce the amount of interfering nodes with minor loss of accuracy.

The contribution in [152] demonstrates that well-defined structures with a finite number of nodes can expediently be applied to represent massive heterogeneous BS topologies. Moreover, these models implicitly yield insights on the number of interferers that mainly determine the characteristics of the interference distribution.

3.2.3 Continuous models

A main merit of stochastic geometry is the transformation of a summation of interference terms into an integration over space by means of the PGFL (conf. Section 3.1). In the context of regular structures, the natural relationship between summation and integration has inspired the so-called *continuous-style approaches*. Those are either *line-* or *area*-based.

In *line-based approaches*, the power of the interferers is uniformly distributed along a line with a certain shape. In [153], the model is constituted by a circle, while in [165], it exhibits a flower-like shape to account for the angle-dependent impact of the interferers, as illustrated in Fig. 5d. While the flower model achieves a better accuracy than the circular model, the evaluation of the results requires a numerical computation. The authors of [165] also show the extension of the flower model to a three-sector setup. The idea is to virtually shift the user position at a certain angle according to the antenna gain.

The *area-based approaches* incorporate *power emission density (PED)*-based models and *fluid* models. The common idea is that the interfering nodes are considered as a continuum of infinitesimal interferers distributed in space. In the *PED-based approach* in [126], each interferer is represented by an individual emitting area, as depicted in Fig. 5e. The receiver of interest is located outside these areas. When arranging the areas in a grid-based fashion, the interference analysis again entails a summation rather than simplifying to integrals. In *fluid models*, the receiver of interested is placed within a ring, which represents a round shaped network around a central cell, as illustrated in Fig. 5f and investigated in [5–7, 158, 166, 167]. The model is shown to yield good approximation for hexagonal transmitter arrangements with both omni- as well as sector antennas [5–7, 158]. The sectorization is incorporated by (i) increasing the interferer density of an omni-directional scenario in proportion to the ratio between the omni-directional-cell surfaces and the sector-cell surfaces, (ii) including the interference from the other sectors belonging to the same site, and (iii) accounting for the impact of the angle-dependent sector antenna gain on the path loss. Remarkably, the authors in [5, 7] show that the OCIF of a *sectorized setup* can be expressed as a linear function of the *omni-directional* one. Noting that the fluid model relies on the hypothesis of a *regular* network, the authors in [167]
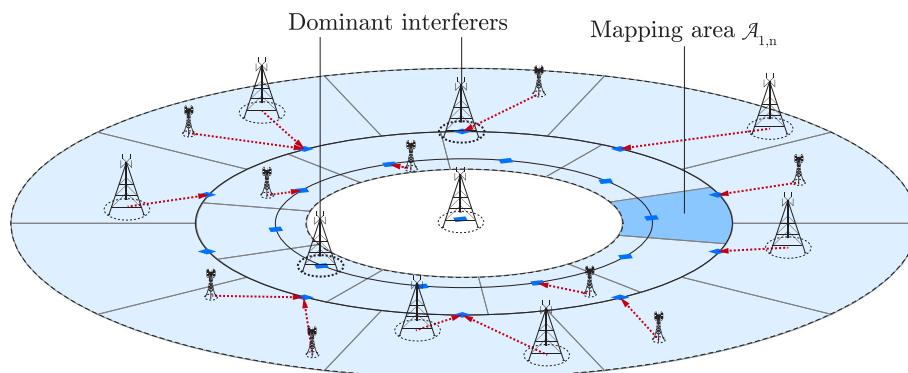

Fig. 6 Circular interference model from [152]. Node locations along the *circles* do not necessarily represent physical sources but rather correspond to mapping points

show its applicability for representing PPP-based models by means of a correction factor. In principle, the fact that the model allows to adjust the transmitter density makes it applicable for representing UDNs. This technique has however not been pursued in literature yet.

Similar to discrete models, a common way to obtain the aggregate interference distribution when using continuous models is to approximate it by a known distribution, as described in Section 3.2.1. Then, the model is mainly used for finding the parameters of the distribution, as demonstrated, e.g., in [5, 153, 166].

3.2.4 Limitations
This section summarizes the limitations of deterministic modeling approaches, most of which were already implicitly discussed above.

- [Finite structures] A frequently stated weakness of deterministic models, and in particular of discrete approaches, is their limitation to represent only *finite* networks with a low number of nodes [1]. Hence, they tend to underestimate the interference. An exception to this issue are fluid models, which allow to specify an infinite outer radius.

- [Approximation by known distribution] In *discrete* models, the PDF of the aggregate interference can be determined by a weighted sum of RVs. With exception to fully symmetric scenarios, in general, this approach does not lead to closed-form results. As discussed in Section 3.2.1, a commonly applied solution is to approximate the interference cPDF by a known distribution. Then, the model is mainly exploited to determine the parameters of the distribution. This technique has also been used in the domain of *continuous* models, as described above. According to Section 3.2.1, there is neither an optimal way to select the PDF nor to calculate its parameters.

- [Representing spatial randomness] Deterministic models are commonly designed to facilitate the geometric treatment of the transmitter locations by either arranging the nodes in a grid-based structure or distributing them over a convenient structure. Hence, they inherently reflect a high degree of *regularity*, with three exceptions:

  1. The node locations of the discrete model represent the transmitters of a practical network. In this case, the interference statistics can only be evaluated via Monte Carlo simulations.
  2. The circular interference model in [152] enables to map arbitrary node locations onto circles with equivalently spaced nodes. The approach has the disadvantage that the mapping needs to be carried out individually for each snapshot of the network.

Thus, it does not allow to represent a general random topology, which is specified only by statistical parameters.

  3. According to [167], the fluid model allows to accurately represent a PPP. The method requires the application of *correction factors*, which are only found empirically via simulations.

A comparison of the discussed interference geometry models is provided in Table 2. It shows whether at least one approach has a tractable interference PDF and whether the model exhibits spatial randomness and spatial correlation, respectively.

3.3 Case study
In this section, the presented transmitter location models are compared against practical outdoor BS deployments by means of a case study. The goal is to evaluate the average interference, which is experienced by a receiver at distance r away from its desired BS. The nodes are assumed to transmit with unit power and to apply universal frequency reuse. The signal propagation is abstracted by a log-distance-dependent path loss law $c^{-1} d^{-4}$, where d denotes the distance between the transmitter and the receiver. Random fading is omitted.

The practical BS deployments are obtained by extracting openly available data from Ofcom's *Sitefinder*[1] for the cities of London and Manchester. The selected area of London has an area of $4\,\mathrm{km}^2$ and counts 319 BSs, yielding an average cell radius of $R_C = 63.17\,\mathrm{m}$ and a BS density of $\mu = 79.75\,10^{-6}\,\mathrm{m}^2$. In the city of Manchester, 37 BSs were counted in a selected area of $1.8\,\mathrm{km}^2$, resulting in $R_C = 125.92\,\mathrm{m}$ and $\mu = 20.56\,\mathrm{m}^2$. The parameters are summarized in Table 3. The results are obtained by uniformly distributing users in the given area, associating them with the closest BS, and determining the aggregate interference as well as their distance to the associated BS.

Table 2 Properties of interference geometry models. *Tractable interference PDF* denotes the fact that at least one approach yields a closed-form solution for the interference PDF

	Tractable interference PDF	Spatial randomness	Spatial correlation
Basic point processes	✓	✓	✗
Cluster point processes	✗	✓	✗
Repulsive point processes	✗	✓	✓
Grid-based model	✓	✗	✓
Practical deployment	✗	✓	✓
Line-based	✗	✗	✓
Area-based	✗	✗	✓

Table 3 BS deployment data as obtained from Ofcom's *Sitefinder* for the cities of London and Manchester

City	London ($A = 4\,km^2$)	Manchester ($A = 1.8\,km^2$)
Number of BSs	319	37
Avg. cell radius	63.17 m	125.92 m

A wrap-around technique is used to avoid interference edge effect.

As a representative for a *stochastic* model (conf. Section 3.1), the hybrid approach from [121] is applied. It comprises a PPP of density μ, where the points of the process are assumed to be excluded from a *guard region* of radius $2R_C$. In order to account for the dominant interferer, a node is randomly placed at the boundary of the guard region, i.e., a circle of radius $2R_C$. In such scenario, the expected interference at distance r is found as

$$\mathbb{E}[I(r)] \approx \frac{1}{c\,(2R_C - r)^\eta} \left(\frac{2\pi\lambda(2R_C - r)^2}{\eta - 2} + 1 \right) \qquad (9)$$

Note that without the guard region, $\mathbb{E}[I(r)]$ does not exist for any value of r [1].

Next to the stochastic model, a discrete and a continuous *deterministic* model (conf. Sections 3.2.1 and 3.2.3) are investigated. The discrete deterministic model is represented by the commonly used hexagonal grid model. The transmitters are spaced out by an inter-site distance of $2R_C$ and are distributed over a circular area of radius $10R_C$. The node at the origin is assumed to be the desired BS. The interference at a certain distance r away from the origin ($0 < r \le R_C$) is obtained by averaging over all angle positions between $-\pi$ and π. The interference from the first tier of interferers is exemplarily given as

$$\mathbb{E}[I(r)] = \int_{-\pi}^{\pi} \frac{1}{2\pi} \sum_{i=1}^{6} \frac{1}{c} \big((2R_C)^2 + r^2 \\ - 4R_C\,r\cos\left(\frac{2\pi}{6}i - \phi \right) \big)^{-\eta/2} d\phi. \qquad (10)$$

The continuous deterministic model is established by a fluid model, as referred from [5]. It comprises an inner radius of $2R_C$ and an outer radius of $10R_C$. According to [5], the interference at distance r is calculated as

$$I = \frac{2\pi\mu c}{\eta - 2} \big((2R_C - r)^{2-\eta} - (10R_C - r)^{2-\eta} \big). \qquad (11)$$

Note that the expressions in Eqs. 9 and 11 for the PPP-based model and the fluid approach are obtained in closed form. The hexagonal grid requires a numerical computation, while the practical models need to be simulated.

Figure 7 shows the average interference power [W] over the distance r of the desired transmitter. The results for the stochastic model as well as the fluid models are obtained by plugging μ and R_C from the practical scenarios into Eqs. 9 and 11, respectively. The results for the hexagonal model are achieved by using the values of R_C as the inter-site distance. It is observed that the grid model yields the largest aggregate interference, while the fluid model exhibits the smallest values. According to [167], both models represent a *regular* distribution of nodes. In the hexagonal model, the dominant nodes are more concentrated at the boundary of the guard region. For this reason, it also yields a larger interference than the PPP-based model, where only a single dominant interferer is located at this boundary. Confirming results in [3], the practical model lies in between the hexagonal grid and the stochastic model, as it exhibits a certain degree of regularity.
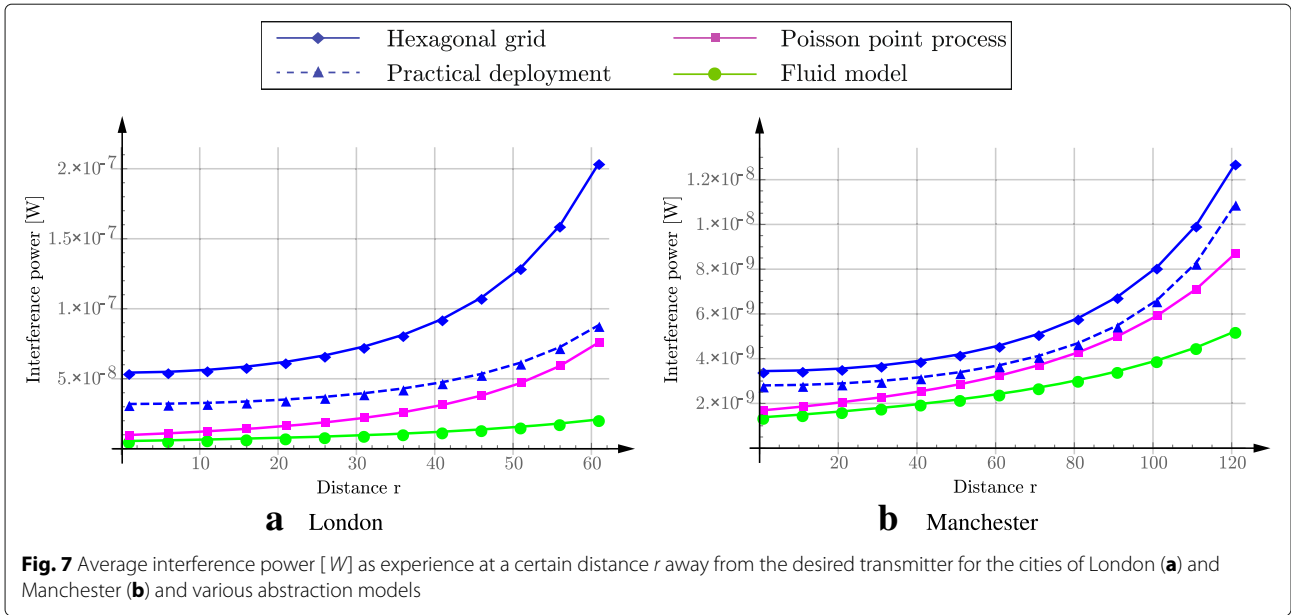
Next to the transmitter locations, the second factor that impacts the interference geometry is the channel access scheme, as discussed in the next section.

3.4 Channel access schemes

In a wireless system, a channel access scheme, frequently referred to as *medium access control (MAC)*, controls a transmitter's admission to use certain resources, e.g., time and frequency. It is either implemented such that each node acts autonomously or in a coordinated manner. In the presence of such scheme, a receiver experiences a *thinned* version of the interference situation. Moreover, a MAC generally introduces correlations among node locations and, thus, considerably complicates the analysis (conf. Section 3.1). Therefore, it is frequently neglected, amounting to the worst case, where all transmitters contribute to the aggregate interference [26, 75, 84, 127, 152, 153]. When a channel access scheme is taken into account in the interference analysis, it commonly falls into one of the following two categories:

- Exlusion region: The MAC is considered to establish an exclusion region around the transmitter-receiver pair, as indicated in Fig. 4. Such regions frequently appear in studies on cognitive radio techniques [92, 168–172].
- Independent thinning: The nodes are assumed to access the resources *randomly and independently of each other*. In the time-domain, this corresponds to the procedures of the Additive Links Online Hawaii Area (ALOHA) protocol [92, 173, 174]. This approach is particularly useful, when the node locations are modeled by a PPP. Then, by virtue of the *thinning property*, applying a random scheme again results in a PPP with different intensity [29].

In the next section, we discuss further aspects of interference analysis.

Fig. 7 Average interference power [*W*] as experience at a certain distance *r* away from the desired transmitter for the cities of London (**a**) and Manchester (**b**) and various abstraction models

4 Further aspects

4.1 Integration

In principle, the abstractions in Section 2 and the models in Section 3 represent independent tools and can thus be combined in an arbitrary fashion. For example, one could apply the hexagonal grid model (conf. Section 3.2.1) for describing the BS locations and the ROP-based blockage model (conf. Section 2.4) together with an empirical path loss law (conf. Eq. 2.3) to characterize the signal propagation. Stochastic blockage models also enable *integrated* frameworks, as demonstrated, e.g., in [55, 67]. In such frameworks, the blockages not only affect the signal propagation but also impact the transmitter locations. As an example, consider transmitters that are restricted to be located outdoors. Then, a transmitter will be kept, if it is not covered by a blockage, and discarded otherwise.

4.2 BS cooperation

BS cooperation is viewed as a key element for interference management in mobile networks [132]. While not directly affecting the large-scale signal propagation nor the BS locations, it impacts whether a signal can be regarded as desired, interfering, or negligible [152, 175, 176].

4.3 Indoor-outdoor partitioning

It is estimated that the majority of today's mobile traffic originates and is consumed indoors [177]. Scenarios consisting of *both indoor and outdoor environments* have not received much attention in analytical studies based on stochastic geometry. With exception of [67], existing approaches mostly neglect the wall partitioning [100, 105]. This mainly stems from the fact that the walls impose inhomogeneities on the signal propagation. The authors of
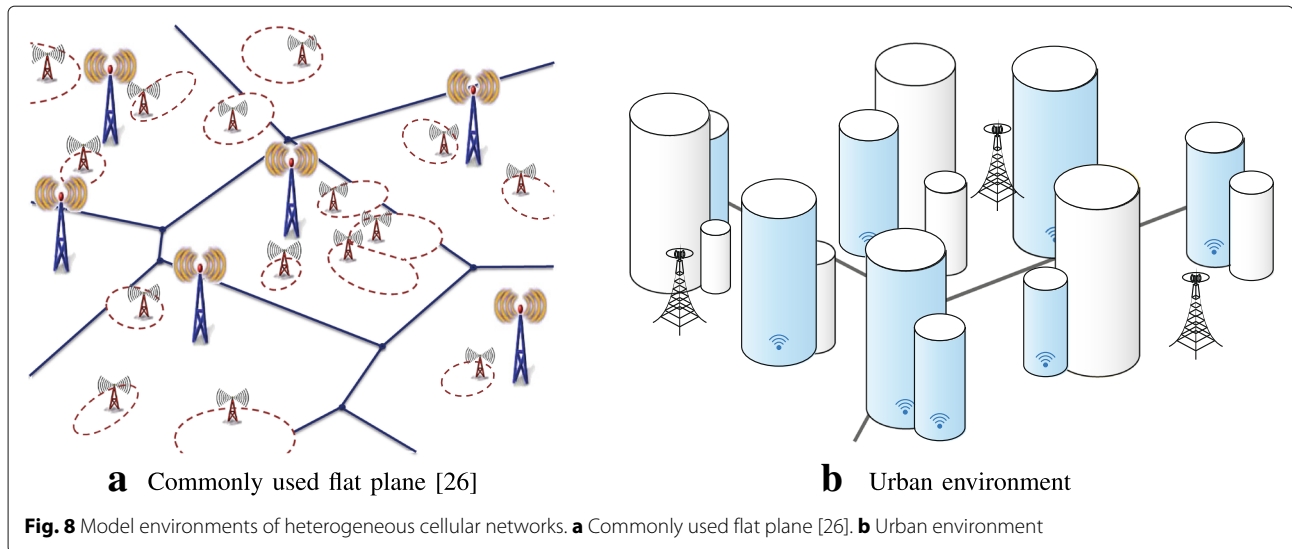
[67] show that the wall partitioning considerably impacts the coverage and rate performance of a typcial indoor user in an urban two-tier heterogeneous cellular network.

4.4 Random displacement

The most tractable results in stochastic geometry are obtained by assuming Rayleigh fading on the desired link. Hence, the modeling environment corresponds to a flat plane without any obstacles, as indicated in Fig. 8a. The characterization of *realistic* signal propagation environments often incorporates a separate *shadowing* term, which is commonly modeled by i.i.d. RVs for simplicity. This model has a very particular impact on the *interference geometry*. In [178], the shadowing RV are argued to act as a *random displacement* of the node locations. It is shown that displacing the nodes of a homogeneous PPP by i.i.d. RV again results in a homogeneous PPP with different intensity. Hence, the spatial distribution of the nodes still exhibits the same characteristics after applying the shadowing, thus not leading to further insights.

4.5 Measuring the goodness of fit

A common method to verify assumptions that simplify the interference analysis is a comparison against Monte Carlo simulations. In order to quantify the *goodness of fit* between the actual interference distribution and its approximation, *non-parametric tests*, also known as *distribution-free inferential method*, are commonly applied [152, 153]. Some of the most frequently used approaches include the *Anderson-Darling test*, the *Cramér-von Mises criterion*, and the *Kolmogorov-Smirnov test*, among others.

Fig. 8 Model environments of heterogeneous cellular networks. **a** Commonly used flat plane [26]. **b** Urban environment

4.6 Exploiting the third spatial dimension

The vast majority of existing abstraction models for both interference geometry and signal propagation is based on the fundamental assumption of *2D* scenarios. With the recent release of a *3D* channel model for the study of elevation beamforming and full-dimension multiple-input multiple-output (MIMO) [41], the 3GPP has made a clear statement for the future of wireless network modeling. A considerable effort should be directed towards augmenting the existing models by a third dimension.

4.7 Millimeter wave transmissions

A framework for modeling blockages, as presented in Section 2.4, currently gains relevance in the study of mmWave transmissions (see, e.g., [179]), where blockages are assumed to have a substantial penetration loss and are therefore assumed to be *impenetrable* [55]. Consequently, they form the so-called LOS regions, as illustrated in Fig. 2. The performance of such network yields a delicate trade-off between blockage and transmitter density [43, 44, 180]. Since the stochastic modeling of transmitters and blockages follows a similar mathematical framework, there combination is a straightforward task. A combined model enables to relate parameters of the network and the environment topology, e.g., transmitter and building density. For example, in [67], this turns out to be particularly useful for evaluating indoor and outdoor coverage.

4.8 Massive MIMO

Studies on massive MIMO transmissions show that other-cell interference may cease to be a major performance-limiting factor in such systems [180, 181]. They follow the intuition that a large array of antennas enables to form

sharp beams such that the desired and the interfering signal establish complementary spaces. Eventually, this may lead to a paradigm shift in the performance analysis of 5G networks, where even the term *cellular* might lose its meaning [179].

5 Conclusions

In this paper, we reviewed path loss attenuation and interference geometry models to characterize aggregate interference statistics in dense urban heterogeneous cellular networks. First, we detailed the characteristics and drawbacks of traditional path loss attenuation models. Then, we focused on stochastic models that represent blockages by means of a random object process. We observed that these models can directly be parameterized by real world data and capture the dependence of blockage effects on the link length. In the context of interference geometry, we observed that discrete models, while representing the most basic method for interference evaluations are also the major obstacle for yielding convenient expressions for the aggregate interference statistics. We showed that various limitations of stochastic approaches, such as interference statistics at eccentric user locations or a certain degree of regularity among the node locations, can be resolved by deterministic structures. It is our hope that this paper provides a comprehensive view on network interference analysis that inspires researchers to develop new frameworks for evaluating the 5G.

Endnote

[1] sitefinder.ofcom.org.uk

Abbreviations

2D: Two-dimensional; 3D: Three-dimensional; 3GPP: 3rd Generation Partnership Project; 5G: Fifth generation of mobile cellular networks; ALOHA: Additive Links On-Line Hawaii Area; AMC: Adaptive modulation and coding;

AWGN: Additive white Gaussian noise; BPP: Binomial point process; BS: Base station; CDF: Cumulative distribution function; CLT: Central limit theorem; CSG: Closed subscriber mode; CDMA: Code-division multiple access; CSMA: Carrier sense multiple access; CF: Characteristic function; D2D: Device-to-device; FAP: Femtocell access point; HCPP: Hardcore point process; HetNet: Heterogeneous network; i.i.d.: Independent and identically distributed; ICI: Inter carrier interference; ISI: Inter symbol interference; LOS: Line of sight; LT: Laplace transform; LTE-A: LTE-advanced; MAC: Medium access control; MAI: Multiple access interference; MCL: Minimum coupling loss; MCL [MCLs]: Minimum coupling losses; MGF: Mobility generating functional; MIMO: Multiple-input multiple-output; mmWave: Millimeter wave; NLOS: Non-line of sight; OCIF: Other-cell interference factor; OFDMA: Orthogonal frequency-division multiple access; OSG: Open subscriber mode; PCP: Poisson cluster process; PDF: Probability density function; PED: Power emission density; PGFL: Probability generating function; PP: Point process; PP [PPs]: Point processes; PPP: Poisson point process; PPP [PPPs]: Poisson point processes; ROP: Random object process; ROP [ROPs]: Random object processes; RV: Random variable; QAM: Quadrature amplitude modulation; SCM: Spatial channel model SIR: Signal-to-interference ratio; SISO: Single-input single-output; SINR: Signal-to-interference-plus-noise ratio; SON: Self-organizing network; TTI: Transmission time interval; UDN: Ultra dense network; UE: User equipment WCDMA: Wideband code division multiple access; Wi-Fi: Wireless Fidelity; WiMAX: Worldwide interoperability for microwave access; WINNER: Wireless World Initiative New Radio

Competing interests
The authors declare that they have no competing interests.

References
1. M Haenggi, RK Ganti, in *Interference in Large Wireless Networks*. Foundations and Trends in Networking, vol. 3 (NoW Publishers, Hanover, 2009)
2. V Chandrasekhar, J Andrews, A Gatherer, Femtocell networks: a survey. IEEE Commun. Mag. **46**(9), 59–67 (2008). doi:10.1109/MCOM.2008.4623708
3. JG Andrews, F Baccelli, RK Ganti, A tractable approach to coverage and rate in cellular networks. IEEE Trans. Commun. **59**(11), 3122–3134 (2011). doi:10.1109/TCOMM.2011.100411.100541
4. F Baccelli, M Klein, M Lebourges, S Zuyev, Stochastic geometry and architecture of communication networks. Telecommun. Syst. **7**, 209–227 (1997). doi:10.1023/A:1019172312328
5. JM Kelif, M Coupechoux, P Godlewski, in *IEEE Wireless Commun. and Networking Conf. (WCNC'08)*. Fluid model of the outage probability in sectored wireless networks, (Las Vegas, USA, 2008), pp. 2933–2938. doi:10.1109/WCNC.2008.513
6. J-M Kelif, M Coupechoux, P Godlewski, A fluid model for performance analysis in cellular networks. EURASIP J. Wireless Commun. Netw. **2010**(1), 435189 (2010). doi:10.1155/2010/435189
7. JM Kelif, in *IEEE Wireless Commun. and Networking Conf. (WCNC'07)*. Multiservice admission on sectored CDMA networks an analytical model, (Kowloon, China, 2007), pp. 3436–3441. doi:10.1109/WCNC.2007.631
8. CC Chan, SV Hanly, Calculating the outage probability in a cdma network with spatial Poisson traffic. IEEE Trans. Veh. Technol. **50**(1), 183–204 (2001). doi:10.1109/25.917918
9. DW Matolak, A Thakur, in *Proc. Southeastern Symp. System Theory*. Outside cell interference dynamics in cellular CDMA, (2003), pp. 148–152. doi:10.1109/SSST.2003.1194547
10. KS Gilhousen, I Jacobs, R Padovani, A Viterbi, J LA Weaver, I CE Wheatley, On the capacity of a cellular CDMA system. IEEE Trans. Veh. Technol. **40**(2), 303–312 (1991). doi:10.1109/25.289411
11. AJ Viterbi, AM Viterbi, KS Gilhousen, E Zehavi, Soft handoff extends CDMA cell coverage and increases reverse link capacity. IEEE J. Sel. Areas Commun. **12**(8), 1281–1288 (1994). doi:10.1109/49.329346
12. R Nasri, A Jaziri, abs/1503.07160. CoRR (2015)
13. M Castaneda, MT Ivrlac, JA Nossek, I Viering, A Klein, in *IEEE Int. Symp. Personal, Indoor and Mobile Radio Commun. (PIMRC'07)*. On downlink intercell interference in a cellular system, (2007), pp. 1–5. doi:10.1109/PIMRC.2007.4394052
14. MK Karray, in *Wireless Days (WD'09)*. Study of a key factor for performance evaluation of wireless cellular networks: the f-factor, (2009), pp. 1–6. doi:10.1109/WD.2009.5449711
15. A Wyner, Shannon-theoretic approach to a Gaussian cellular multiple-access channel. IEEE Trans. Inf. Theory. **40**(6), 1713–1727 (1994). doi:10.1109/18.340450
16. J Gertner, *The Idea Factory: Bell Labs and the Great Age of American Innovation*. (Penguin Publishing Group, New York, 2012)
17. NC Beaulieu, AA Abu-Dayya, Bandwidth efficient QPSK in cochannel interference and fading. IEEE Trans. Commun. **43**(9), 2464–2474 (1995)
18. J Cheng, NC Beaulieu, Accurate DS-CDMA bit-error probability calculation in Rayleigh fading. IEEE Trans. Wireless Commun. **1**(1), 3–15 (2002)
19. A Giorgetti, M Chiani, Influence of fading on the Gaussian approximation for BPSK and QPSK with asynchronous cochannel interference. IEEE Trans. Wireless Commun. **4**(2), 384–389 (2005)
20. M Aljuaid, H Yanikomeroglu, in *Biennial Symp. Commun. (QBSC)*. Investigating the validity of the Gaussian approximation for the distribution of the aggregate interference power in large wireless networks, (Kingston, ON, Canada, 2010), pp. 122–125. doi:10.1109/BSC.2010.5472989
21. D Middleton, Non-Gaussian noise models in signal processing for telecommunications: new methods and results for class A and class B noise models. IEEE Trans. Inf. Theory, 1129–1149 (1999)
22. H Inaltekin, M Chiang, HV Poor, SB Wicker, On unbounded path-loss models: effects of singularity on wireless network performance. IEEE J. Sel. Areas Commun. **27**(7), 1078–1092 (2009)
23. A Rabbachin, TQ Quek, H Shin, MZ Win, Cognitive network interference. IEEE J. Sel. Areas Commun. **29**(2), 480–493 (2011)
24. P Carr, H Geman, DB Madan, M Yor, The fine structure of asset returns: an empirical investigation. J. Bus. **75**(2), 305–333 (2002)
25. M Derakhshani, T Le-Ngoc, Aggregate interference and capacity-outage analysis in a cognitive radio network. IEEE Trans. Veh. Technol. **61**(1), 196–207 (2012)
26. H ElSawy, E Hossain, M Haenggi, Stochastic geometry for modeling, analysis, and design of multi-tier and cognitive cellular wireless networks: a survey. IEEE Commun. Surveys Tutor. **15**(3), 996–1019 (2013)
27. B Pijcke, M Zwingelstein-Colin, M Gazalet, M Gharbi, P Corlay, An analytical model for the intercell interference power in the downlink of wireless cellular networks. EURASIP J. Wireless Commun. Netw. **2011**(1), 95 (2011). doi:10.1186/1687-1499-2011-95
28. JG Andrews, RK Ganti, M Haenggi, N Jindal, S Weber, A primer on spatial modeling and analysis in wireless networks. IEEE Commun. Mag. **48**(11), 156–163 (2010)
29. F Baccelli, B Blaszczyszyn, *Stochastic Geometry and Wireless Networks: Volume I Theory. ser. Foundation and Trends in Networking*. (Now Publishers, 2009), pp. 249–449. doi:10.1561/1300000006
30. MZ Win, PC Pinto, LA Shepp, A mathematical theory of network interference and its applications. Proc. IEEE. **97**(2), 205–230 (2009)
31. K Gulati, BL Evans, JG Andrews, KR Tinsley, Statistics of co-channel interference in a field of Poisson and Poisson-Poisson clustered interferers. IEEE Trans. Signal Process. **58**(12), 6207–6222 (2010)
32. M Kountouris, N Pappas, in *Int. Symp. Wireless Commun. Syst. (ISWCS)*. Approximating the interference distribution in large wireless networks, (Barcelona, Spain, 2014)
33. M Haenggi, JG Andrews, F Baccelli, O Dousse, M Franceschetti, Stochastic geometry and random graphs for the analysis and design of wireless networks. IEEE J. Sel. Areas Commun. **27**(7), 1029–1046 (2009). doi:10.1109/JSAC.2009.090902
34. D Avidor, S Mukherjee, Hidden issues in the simulation of fixed wireless systems. Wireless Networks. **7**(2), 187–200 (2001). doi:10.1023/A:1016641723805
35. F Baccelli, B Blaszczyszyn, *Stochastic Geometry and Wireless Networks, Volume II - Applications. ser. Foundations and Trends in Networking*, vol. 2. (NoW Publishers, 2009), p. 209. doi:10.1561/1300000026

36. X Yang, G de Veciana, Inducing multiscale clustering using multistage MAC contention in CDMA ad hoc networks. IEEE/ACM Trans. Netw. **15**(6), 1387–1400 (2007). doi:10.1109/TNET.2007.902690

37. C Phillips, D Sicker, D Grunwald, A survey of wireless path loss prediction and coverage mapping methods. IEEE Commun. Surv. Tutor. **15**(1), 255–270 (2013). doi:10.1109/SURV.2012.022412.00172

38. JB Andersen, TS Rappaport, S Yoshida, Propagation measurements and models for wireless communications channels. IEEE Commun. Mag. **33**(1), 42–49 (1995). doi:10.1109/35.339880

39. 3rd Generation Partnership Project (3GPP), Spatial channel model for multiple input multiple output (MIMO) simulations (2012). TR 325.996, 3rd Generation Partnership Project (3GPP)

40. WINNER II WP1, WINNER II channel models (2007). IST-4-027756 WINNER II Deliverable D1.1.2

41. 3rd Generation Partnership Project (3GPP), Study on 3D channel model for LTE (2014). TR 36.873, 3rd Generation Partnership Project (3GPP)

42. MD Renzo, Stochastic geometry modeling and analysis of multi-tier millimeter wave cellular networks. IEEE Trans. Wireless Commun. **14**(9), 5038–5057 (2015). doi:10.1109/TWC.2015.2431689

43. T Bai, RW Heath Jr., in *IEEE Global Conf. Signal and Inform. Process. (GlobalSIP)*. Coverage analysis for millimeter wave cellular networks with blockage effects, (Austin, TX, USA, 2013), pp. 727–730. doi:10.1109/GlobalSIP.2013.6736994

44. T Bai, A Alkhateeb, R Heath, Coverage and capacity of millimeter-wave cellular networks. IEEE Commun. Mag. **52**(9), 70–77 (2014). doi:10.1109/MCOM.2014.6894455

45. RWHJ Kiran Venugopal, MC Valenti, in *Information Theory and Applications (ITA)*. Interference in Finite-Sized Highly Dense Millimeter Wave Networks, (San Diego, CA, USA, 2015)

46. M Gholizadeh, H Amindavar, J Ritcey, On the capacity of MIMO correlated Nakagami-m fading channels using copula. EURASIP J. Wireless Commun. Network. **2015**(1), 138 (2015). doi:10.1186/s13638-015-0369-3

47. J Hu, NC Beaulieu, Accurate simple closed-form approximations to Rayleigh sum distributions and densities. IEEE Commun. Lett. **9**(2), 109–111 (2005)

48. CA Coelho, The generalized integer Gamma distribution—a basis for distributions in multivariate statistics. J. Multivariate Anal. **64**(1), 86–102 (1998). doi:10.1006/jmva.1997.1710

49. K Zheng, L Zhao, J Mei, B Shao, W Xiang, L Hanzo, Survey of large-scale MIMO systems. IEEE Commun. Surv. Tutor. **17**(3), 1738–1760 (2015). doi:10.1109/COMST.2015.2425294

50. COST Action 231, Digital mobile radio towards future generation systems, final report (1999). tech. rep. EUR 18957, European Communities

51. D Skraparlis, V Sakarellos, A Panagopoulos, J Kanellopoulos, Outage performance analysis of cooperative diversity with MRC and SC in correlated lognormal channels. EURASIP J. Wireless Commun. Netw. **2009**(1), 707839 (2009). doi:10.1155/2009/707839

52. X Zhang, M Haenggi, A stochastic geometry analysis of inter-cell interference coordination and intra-cell diversity. IEEE Trans. Wireless Commun. **13**(12), 6655–6669 (2014)

53. U Schilcher, C Bettstetter, G Brandner, Temporal correlation of interference in wireless networks with Rayleigh block fading. IEEE Trans. Mobile Comput. **11**(12), 2109–2120 (2012). doi:10.1109/TMC.2011.244

54. F Baccelli, X Zhang, in *IEEE Conf. Comput. Commun. (INFOCOM)*. A correlated shadowing model for urban wireless networks, (2015), pp. 801–809. doi:10.1109/INFOCOM.2015.7218450

55. T Bai, R Vaze, Heath Jr, RW, Analysis of blockage effects on urban cellular networks. IEEE Trans. Wireless Commun. **13**(9), 5070–5083 (2014). doi:10.1109/TWC.2014.2331971

56. 3rd Generation Partnership Project (3GPP), Evolved Universal Terrestrial Radio Access (E-UTRA); Further Advancements for E-UTRA Physical Layer Aspects (2010). TR 36.814, 3rd Generation Partnership Project (3GPP)

57. X Zhang, JG Andrews, Downlink cellular network analysis with multi-slope path loss models. IEEE Trans. Commun. **63**(5), 1881–1894 (2015). doi:10.1109/TCOMM.2015.2413412

58. M Ding, P Wang, Ló,pez-Pérez, G Mao, Z Lin, Performance impact of LoS and NLoS transmissions in small cell networks. CoRR. **abs/1503.04251** (2015)

59. D Li, J Wang, M Chen, Z Zhang, Z Li, Base-band involved integrative modeling for studying the transmission characteristics of wireless link in railway environment. EURASIP J. Wireless Commun. Netw. **2015**(1), 81 (2015)

60. S-H Liao, C-H Chen, C-C Chiu, M-H Ho, T Wysocki, B Wysocki, Optimal receiver antenna location in indoor environment using dynamic differential evolution and genetic algorithm. EURASIP J. Wireless Commun. Netw. **2013**(1), 235 (2013). doi:10.1186/1687-1499-2013-235

61. JF Monserrat, JC Sa1l Inca, D Martn-Sacristn, Map-based channel model for urban macrocell propagation scenarios. Int. J. Antennas Propag. **2015**(1), 5 (2015). doi:10.1155/2015/172501

62. H-S Jo, P Xia, JG Andrews, Open, closed, and shared access femtocells in the downlink. EURASIP J. Wireless Commun. Netw. **2012**(1) (2012). doi:10.1186/1687-1499-2012-363

63. K Sung, H Haas, S McLaughlin, A semianalytical PDF of downlink SINR for femtocell networks. EURASIP J. Wireless Commun. Netw. **2010**(1), 256370 (2010). doi:10.1155/2010/256370

64. SN Chiu, D Stoyan, WS Kendall, J Mecke, *Stochastic Geometry and Its Applications, ser. Wiley Series in Probability and Statistics*. (Wiley, 2013)

65. TS Rappaport, S Deng, in *Communication Workshop (ICCW), 2015 IEEE International Conference On*. 73 GHz wideband millimeter-wave foliage and ground reflection measurements and models, (2015), pp. 1238–1243. doi:10.1109/ICCW.2015.7247347

66. T Bai, R Vaze, RW Heath Jr., in *Int. Conf. Signal Process. and Commun. (SPCOM)*. Using random shape theory to model blockage in random cellular networks, (Bangalore, India, 2012). doi:10.1109/SPCOM.2012.6290250

67. M Taranetz, M Rupp, Heath Jr, RW, T Bai, in *Proc. Int. Symp. Wireless Commun. Syst. (ISWCS'14)*. Analysis of small cell partitioning in urban two-tier heterogeneous cellular networks, (Barcelona, Spain, 2014)

68. T Bai, RW Heath, Coverage and rate analysis for millimeter-wave cellular networks. IEEE Trans. Wireless Commun. **14**(2), 1100–1114 (2015). doi:10.1109/TWC.2014.2364267

69. J Ruiz Aviles, M Toril, S Luna-Ramirez, A femtocell location strategy for improving adaptive traffic sharing in heterogeneous LTE networks. EURASIP J. Wireless Commun. Netw. **2015**(1), 38 (2015). doi:10.1186/s13638-015-0246-0

70. M Simsek, M Bennis, I Guvenc, Mobility management in hetnets: a learning-based perspective. EURASIP J. Wireless Commun. Netw. **2015**(1), 26 (2015). doi:10.1186/s13638-015-0244-2

71. V Fernandez-Lopez, K Pedersen, B Soret, Interference characterization and mitigation benefit analysis for LTE-A macro and small cell deployments. EURASIP J. Wireless Commun. Netw. **2015**(1), 110 (2015). doi:10.1186/s13638-015-0344-z

72. A Guo, M Haenggi, Spatial stochastic models and metrics for the structure of base stations in cellular networks. IEEE Trans. Wireless Commun. **12**(11), 5800–5812 (2013)

73. JG Andrews, H Claussen, M Dohler, S Rangan, MC Reed, Femtocells: Past, present, and future. IEEE J. Sel. Areas Commun. **30**(3), 497–508 (2012). doi:10.1109/JSAC.2012.120401

74. V Chandrasekhar, JG Andrews, Uplink capacity and interference avoidance for two-tier femtocell networks. IEEE Trans. Wireless Commun. **8**(7), 3498–3509 (2009). doi:10.1109/TWC.2009.070475

75. A Ghosh, N Mangalvedhe, R Ratasuk, B Mondal, M Cudak, E Visotsky, TA Thomas, JG Andrews, P Xia, HS Jo, et al, Heterogeneous cellular networks: from theory to practice. IEEE Commun. Mag. **50**(6), 54–64 (2012)

76. JG Andrews, Seven ways that HetNets are a cellular paradigm shift. IEEE Commun. Mag. **51**(3), 136–144 (2013). doi:10.1109/MCOM.2013.6476878

77. C-H Lee, C-Y Shih, Y-S Chen, Stochastic geometry based models for modeling cellular networks in urban areas. Wireless Netw. **19**(6), 1063–1072 (2013). doi:10.1007/s11276-012-0518-0

78. JA Mcfadden, The entropy of a point process. J. Soc. for Ind. Appl. Math. **13**(4), 988–994 (1965). doi:10.2307/2946418

79. E Bastug, M Bennis, M Kountouris, M Debbah, Cache-enabled small cell networks: modeling and tradeoffs. EURASIP J. Wireless Commun. Netw. **2015**(1), 41 (2015). doi:10.1186/s13638-015-0250-4

80. F Baccelli, S Zuyev, in *Frontiers in Queueing: Models and Applications in Science and Engineering*. Stochastic geometry models of mobile communication networks (CRC Press, Inc, Boca Raton, 1996), pp. 227–243

81. TX Brown, Cellular performance bounds via shotgun cellular systems. IEEE J. Sel. Areas Commun. **18**(11), 2443–2455 (2000). doi:10.1109/49.895048

82. C Ren, J Zhang, W Xie, D Zhang, in *Int. Conf. Inform. Sci. and Technol. (ICIST)*. Performance analysis for heterogeneous cellular networks based

on Matern-like point process model, (Yangzhou, China, 2013), pp. 1507–1511. doi:10.1109/ICIST.2013.6747823

83. M Di Renzo, A Guidotti, GE Corazza, Average rate of downlink heterogeneous cellular networks over generalized fading channels: a stochastic geometry approach. IEEE Trans. Commun. **61**(7), 3050–3071 (2013)

84. M Haenggi, *Stochastic Geometry for Wireless Networks, ser. Stochastic Geometry for Wireless Networks*. (Cambridge University Press, 2012). http://books.google.de/books?id=t8FeLgEACAAJ

85. S Weber, JG Andrews, Transmission capacity of wireless networks. Foundations Trends Netw. **5**(2–3), 109–281 (2012). doi:10.1561/1300000032

86. N Campbell, Discontinuities in light emission. Proc. Cambridge Philosoph. Soc., Math. and Physical Sci. **15**, 310–328 (1909)

87. N Campbell, The study of discontinuous phenomena. Proc. Cambridge Philosoph. Soc., Math. and Physical Sci. **15**, 117–136 (1909)

88. W Schottky, ber spontane Stromschwankungen in verschiedenen Elektrizittsleitern. Annalen der Physik. **362**(23), 541–567 (1918)

89. SO Rice, Mathematical analysis of random noise. Bell Syst. Tech. J. **23**(3), 282–332 (1944)

90. EJG Pitman, EJ Williams, *Studies in Probability and Statistics : Papers in Honour of Edwin J. G. Pitman*. (North-Holland Pub. Co, 1976)

91. ES Sousa, JA Silvester, Optimum transmission ranges in a direct-sequence spread-spectrum multihop packet radio network. IEEE J. Sel. Areas Commun. **8**(5), 762–771 (1990)

92. F Panahi, T Ohtsuki, Stochastic geometry modeling and analysis of cognitive heterogeneous cellular networks. EURASIP J. Wireless Commun. Netw. **2015**(1), 141 (2015). doi:10.1186/s13638-015-0363-9

93. Y Wang, Y Zhang, Y Chen, R Wei, Energy-efficient design of two-tier femtocell networks. EURASIP J. Wireless Commun. Netw. **2015**(1), 40 (2015). doi:10.1186/s13638-015-0242-4

94. J Xu, J Zhang, JG Andrews, On the accuracy of the Wyner model in cellular networks. IEEE Trans. Wireless Commun. **10**(9), 3098–3109 (2011). doi:10.1109/TWC.2011.062911.100481

95. F Baccelli, B Blaszczyszyn, P Muhlethaler, Stochastic analysis of spatial and opportunistic ALOHA. IEEE J. Sel. Areas Commun. **27**(7), 1105–1119 (2009). doi:10.1109/JSAC.2009.090908

96. HS Dhillon, RK Ganti, F Baccelli, JG Andrews, Modeling and analysis of K-tier downlink heterogeneous cellular networks. IEEE J. Sel. Areas Commun. **30**(3), 550–560 (2012). doi:10.1109/JSAC.2012.120405

97. H-S Jo, YJ Sang, P Xia, JG Andrews, Heterogeneous cellular networks with flexible cell association: A comprehensive downlink SINR analysis. IEEE Trans. Wireless Commun. **11**(10), 3484–3495 (2012). doi:10.1109/TWC.2012.081612.111361

98. S Mukherjee, Distribution of downlink SINR in heterogeneous cellular networks. IEEE J. Sel. Areas Commun. **30**(3), 575–585 (2012)

99. WC Cheung, TQ Quek, M Kountouris, Throughput optimization, spectrum allocation, and access control in two-tier femtocell networks. IEEE J. Sel. Areas Commun. **30**(3), 561–574 (2012)

100. H ElSawy, E Hossain, Two-tier HetNets with cognitive femtocells: downlink performance modeling and analysis in a multichannel environment. IEEE Trans. Mobile Comput. **13**(3), 649–663 (2014). doi:10.1109/TMC.2013.36

101. H ElSawy, E Hossain, in *Int. Symp. Modeling Optimization in Mobile, Ad Hoc Wireless Networks*. On cognitive small cells in two-tier heterogeneous networks, (Tsukuba Science City, Japan, 2013), pp. 75–82

102. C-H Lee, M Haenggi, Interference and outage in Poisson cognitive networks. IEEE Trans. Wireless Commun. **11**(4), 1392–1401 (2012). doi:10.1109/TWC.2012.021512.110131

103. V Chandrasekhar, JG Andrews, Spectrum allocation in tiered cellular networks. IEEE Trans. Commun. **57**(10), 3059–3068 (2009)

104. P Brémaud, *Mathematical principles of signal processing: Fourier and wavelet analysis*. (Springer, New York, 2002)

105. V Chandrasekhar, JG Andrews, in *IEEE Global Telecommun. Conf*. Uplink capacity and interference avoidance for two-tier cellular networks, (Washington, DC, USA, 2007), pp. 3322–3326. doi:10.1109/GLOCOM.2007.630

106. PC Pinto, A Giorgetti, MZ Win, M Chiani, A stochastic geometry approach to coexistence in heterogeneous wireless networks. IEEE J. Sel. Areas Commun. **27**(7), 1268–1282 (2009). doi:10.1109/JSAC.2009.090922

107. G Alfano, M Garetto, E Leonardi, in *IEEE Int. Conf. Comput. Commun. (INFOCOM)*. New insights into the stochastic geometry analysis of dense CSMA networks, (Shanghai, China, 2011), pp. 2642–2650. doi:10.1109/INFCOM.2011.5935092

108. HS Dhillon, RK Ganti, F Baccelli, JG Andrews, in *Allerton Conf. Commun., Control, and Computing 2011 (Allerton)*. Coverage and ergodic rate in K-tier downlink heterogeneous cellular networks, (Monticello, IL, USA, 2011), pp. 1627–1632. doi:10.1109/Allerton.2011.6120363

109. G Alfano, M Garetto, E Leonardi, New directions into the stochastic geometry analysis of dense csma networks. IEEE Trans. Mobile Comput. **13**(2), 324–336 (2014). doi:10.1109/TMC.2012.248

110. M Haenggi, The Meta Distribution of the SIR in Poisson Bipolar and Cellular Networks (2015). http://arxiv.org/abs/1506.01644

111. A Tukmanov, Z Ding, S Boussakta, A Jamalipour, On the impact of network geometric models on multicell cooperative communication systems. IEEE Wireless Commun. IEEE. **20**(1), 75–81 (2013). doi:10.1109/MWC.2013.6472202

112. RK Ganti, M Haenggi, Spatial and temporal correlation of the interference in ALOHA ad hoc networks. IEEE Commun. Lett. IEEE. **13**(9), 631–633 (2009). doi:10.1109/LCOMM.2009.090837

113. M Haenggi, Mean interference in hard-core wireless networks. IEEE Commun. Lett. **15**(8), 792–794 (2011). doi:10.1109/LCOMM.2011.061611.110960

114. H ElSawy, E Hossain, S Camorlinga, in *OEEE Int. Conf. Commun. (ICC)*. Characterizing random CSMA wireless networks: a stochastic geometry approach, (2012), pp. 5000–5004. doi:10.1109/ICC.2012.6363772

115. J Møller, ML Huber, RL Wolpert, Perfect simulation and moment properties for the matérn type {III} process. Stochastic Process. Appl. **120**(11), 2142–2158 (2010). doi:10.1016/j.spa.2010.06.002

116. ML Huber, RL Wolpert, Likelihood-based inference for matérn type-iii repulsive point processes. Advances in Applied Probability, 958–977 (2009)

117. U Schilcher, M Gyarmati, C Bettstetter, YW Chung, YH Kim, in *Veh. Technol. Conf. (VTC Spring)*. Measuring inhomogeneity in spatial distributions, (Singapore, 2008), pp. 2690–2694. doi:10.1109/VETECS.2008.589

118. BD Ripley, *Spatial Statistics*, vol. 575. (John Wiley & Sons, 2005)

119. E Marcon, F Puech, Generalizing Ripley's K function to inhomogeneous populations. HAL-SHS (2009)

120. PM Dixon, in *Encyclopedia of Environmetrics*. Ripley's K function (John Wiley & Sons, Ltd, 2001). http://dx.doi.org/10.1002/9780470057339.var046

121. Heath Jr, RW, M Kountouris, T Bai, Modeling heterogeneous network interference using Poisson point processes. IEEE Trans. Signal Process. **61**(16), 4114–4126 (2013). doi:10.1109/TSP.2013.2262679

122. Heath Jr, RW, M Kountouris, in *Inf. Theory and Appl. Workshop (ITA)*. Modeling heterogeneous network interference, (San Diego, CA, USA, 2012), pp. 17–22. doi:10.1109/ITA.2012.6181825

123. A Kliks, J Perez-Romero, L Boukhatem, A Zalonis, Technical advances in the design and deployment of future heterogeneous networks. EURASIP J. Wireless Commun. Netw. **2015**(1), 153 (2015). doi:10.1186/s13638-015-0396-0

124. S Fan, H Tian, C Sengul, Self-optimized heterogeneous networks for energy efficiency. EURASIP J. Wireless Commun. Netwo. **2015**(1), 21 (2015). doi:10.1186/s13638-015-0261-1

125. J Fernandez-Segovia, S Luna-Ramirez, M Toril, A Vallejo-Mora, C Ubeda, A computationally efficient method for self-planning uplink power control parameters in lte. EURASIP J. Wireless Commun. Netw. **2015**(1), 80 (2015). doi:10.1186/s13638-015-0320-7

126. M Ni, J Pan, L Cai, in *Communications (ICC), 2014 IEEE International Conference On*. Power emission density-based interference analysis for random wireless networks, (2014), pp. 440–445. doi:10.1109/ICC.2014.6883358

127. F Iqbal, M Javed, A Naveed, Interference-aware multipath routing in wireless mesh network. EURASIP J. Wireless Commun. Netw. **2014**(1), 140 (2014). doi:10.1186/1687-1499-2014-140

128. K-H Hui, W Lau, O Yue, Partial interference and its performance impact on wireless multiple access networks. EURASIP J. Wireless Commun. Netw. **2010**(1), 735083 (2010). doi:10.1155/2010/735083

129. G Calcev, J Bonta, OFDMA cellular networks with opportunistic two-hop relays. EURASIP J. Wireless Commun. Netw. **2009**(1), 702659 (2009). doi:10.1155/2009/702659

130. K Doppler, S Redana, M Wodczak, P Rost, R Wichman, Dynamic resource assignment and cooperative relaying in cellular networks: Concept and

performance assessment. EURASIP J. Wireless Commun. Netw. **2009**(1), 475281 (2009). doi:10.1155/2009/475281

131. P Pirinen, Outage analysis of ultra-wideband system in lognormal multipath fading and square-shaped cellular configurations. EURASIP J. Wireless Commun. Netw. **2006**(1), 019460 (2006). doi:10.1155/WCN/2006/19460

132. A Lozano, Heath Jr, RW, JG Andrews, Fundamental limits of cooperation. IEEE Trans. Inf. Theory. **59**(9), 5213–5226 (2013). doi:10.1109/TIT.2013.2253153

133. F Letourneux, Y Corre, E Suteau, Y Lostanlen, 3D coverage analysis of LTE urban heterogeneous networks with dense femtocell deployments. EURASIP J. Wireless Commun. Netw. **2012**(1), 319 (2012). doi:10.1186/1687-1499-2012-319

134. R Kurda, L Boukhatem, M Kaneko, Femtocell power control methods based on users' contes xt information in two-tier heterogeneous networks. EURASIP J. Wireless Commun. Netw. **2015**(1), 129 (2015). doi:10.1186/s13638-015-0328-z

135. J Wu, S Jin, L Jiang, G Wang, Dynamic switching off algorithms for pico base stations in heterogeneous cellular networks. EURASIP J. Wireless Commun. Netw. **2015**(1), 117 (2015). doi:10.1186/s13638-015-0280-y

136. A Chiumento, S Pollin, C Desset, L der Perre, R Lauwereins, Scalable HetNet interference management and the impact of limited channel state information. EURASIP J. Wireless Commun. Netw. **2015**(1), 74 (2015). doi:10.1186/s13638-015-0283-8

137. M-S Alouini, A Abdi, M Kaveh, Sum of Gamma variates and performance of wireless communication systems over Nakagami-fading channels. IEEE Trans. Veh. Technol. **50**(6), 1471–1480 (2001). doi:10.1109/25.966578

138. VA Aalo, T Piboongungon, GP Efthymoglou, Another look at the performance of MRC schemes in Nakagami-m fading channels with arbitrary parameters. IEEE Trans. Commun. **53**(12), 2002–2005 (2005). doi:10.1109/TCOMM.2005.860089

139. IS Ansari, F Yilmaz, M-S Alouini, O Kucur, in *IEEE Int. Workshop Signal Process. Advances in Wireless Commun. (SPAWC)*. On the sum of Gamma random variates with application to the performance of maximal ratio combining over Nakagami-m fading channels, (Cesme, Turkey, 2012), pp. 394–398

140. TA Tsiftsis, GK Karagiannidis, SA Kotsopoulos, NC Sagias, in *Int. Symp. Commun. Syst., Networks and Digital Signal Process. (CSNDSP)*. Performance of MRC diversity receivers over correlated Nakagami-*m* fading channels, (Patras, Greece, 2006)

141. GK Karagiannidis, NC Sagias, TA Tsiftsis, Closed-form statistics for the sum of squared Nakagami-m variates and its applications. IEEE Trans. Commun. **54**(8), 1353–1359 (2006). doi:10.1109/TCOMM.2006.878812

142. GP Efthymoglou, T Piboongungon, VA Aalo, Performance of DS-CDMA receivers with MRC in Nakagami-m fading channels with arbitrary fading parameters. IEEE Trans. Veh. Technol. **55**(1), 104–114 (2006). doi:10.1109/TVT.2005.861204

143. L-L Yang, H-H Chen, Error probability of digital communications using relay diversity over Nakagami-m fading channels. IEEE Trans. Wireless Commun. **7**(5), 1806–1811 (2008)

144. DJ Torrieri, MC Valenti, The outage probability of a finite ad hoc network in Nakagami fading. IEEE Trans. Commun. **60**(11), 3509–3518 (2012)

145. PG Moschopoulos, The distribution of the sum of independent Gamma random variables. Ann. Inst. Statist. Math. **37**(1), 541–544 (1985)

146. DG Kabe, On the exact distribution of a class of multivariate test criteria. Ann. Math. Statist. **33**(3), 1197–1200 (1962)

147. EM Scheuer, Reliability of an m-out-of-n system when component failure induces higher failure rates in survivors. IEEE Trans. Rel. **37**(1), 73–74 (1988). doi:10.1109/24.3717

148. SV Amari, RB Misra, Closed-form expressions for distribution of sum of exponential random variables. IEEE Trans. Rel. **46**(4), 519–522 (1997). doi:10.1109/24.693785

149. AA Abu-Dayya, NC Beaulieu, Outage probabilities in the presence of correlated lognormal interferers. IEEE Trans. Veh. Technol. **43**(1), 164–173 (1994)

150. NC Beaulieu, AA Abu-Dayya, PJ McLane, Estimating the distribution of a sum of independent lognormal random variables. IEEE Trans. Commun. **43**(12), 2869–2873 (1995)

151. NB Mehta, J Wu, AF Molisch, J Zhang, Approximating a sum of random variables with a lognormal. IEEE Trans. Wireless Commun. **6**(7), 2690–2699 (2007)

152. M Taranetz, M Rupp, A circular interference model for heterogeneous cellular networks. IEEE Trans. Wireless Commun. **15**, 1432–1444 (2015). doi:10.1109/TWC.2015.2490068

153. M Taranetz, M Rupp, in *Proc. Int. Wireless Commun. & Mobile Computing Conf.* A circular interference model for wireless cellular networks, (Nicosia, Cyprus, 2014)

154. KB Baltzis. Cellular Networks - Positioning, Performance Analysis, Reliability (InTech, 2011). doi:10.5772/626

155. Y Zhuang, Y Luo, L Cai, J Pan, in *IEEE Global Telecommun. Conf. (GLOBECOM)*. A geometric probability model for capacity analysis and interference estimation in wireless mobile cellular systems, (Houston, TX, USA, 2011). doi:10.1109/GLOCOM.2011.6134503

156. NC Beaulieu, Q Xie, An optimal lognormal approximation to lognormal sum distributions. IEEE Trans. Veh. Technol. **53**(2), 479–489 (2004). doi:10.1109/TVT.2004.823494

157. JCS Filho, MD Yacoub, P Cardieri, Highly accurate range-adaptive lognormal approximation to lognormal sum distributions. Electron. Lett. **42**(6), 361–363 (2006). doi:10.1049/el:20064091

158. D Ben Cheikh, J-M Kelif, M Coupechoux, P Godlewski, SIR distribution analysis in cellular networks considering the joint impact of path-loss, shadowing and fast fading. EURASIP J. Wireless Commun. Networking. **2011**(1) (2011). doi:10.1186/1687-1499-2011-137

159. M Aljuaid, H Yanikomeroglu, Investigating the Gaussian convergence of the distribution of the aggregate interference power in large wireless networks. IEEE Trans. Veh. Technol. **59**(9), 4418–4424 (2010)

160. RK Ganti, M Haenggi, in *IEEE Int. Symp. Inf. Theory (ISIT)*. Interference in ad hoc networks with general motion-invariant node distributions, (Toronto, ON, Canada, 2008). doi:10.1109/ISIT.2008.4594936

161. AC Berry, The accuracy of the Gaussian approximation to the sum of independent variates. Trans. Amer. Mathem. Soc. **49**(1), 122–136 (1941)

162. PA Dmochowski, PJ Smith, M Shafi, JG Andrews, R Mehta, in *IEEE Int. Conf. Commun. (ICC)*. Interference models for heterogenous sources, (Ottawa, ON, Canada, 2012), pp. 4049–4054. doi:10.1109/ICC.2012.6364627

163. Heath Jr, RW, T Wu, YH Kwon, ACK Soong, Multiuser MIMO in distributed antenna systems with out-of-cell interference. IEEE Trans. Signal Process. **59**(10), 4885–4899 (2011). doi:10.1109/TSP.2011.2161985

164. S Kusaladharma, C Tellambura, Aggregate interference analysis for underlay cognitive radio networks. IEEE Wireless Commun. Lett. **1**(6), 641–644 (2012). doi:10.1109/WCL.2012.091312.120600

165. B Almeroth, AJ Fehske, G Fettweis, E Zimmermann, in *IEEE GLOBECOM Workshops*. Analytical interference models for the downlink of a cellular mobile network, (2011), pp. 739–743. doi:10.1109/GLOCOMW.2011.6162552

166. R Combes, J-M Kelif, in *IEEE Conf. Commun. (ICC)*. A justification of the fluid network model using stochastic geometry, (2013), pp. 6174–6178. doi:10.1109/ICC.2013.6655593

167. JM Kelif, Sé,nécal, C Bridon, M Coupechoux, A fluid approach for poisson wireless networks. CoRR. **abs/1401.6336** (2014)

168. P Lan, L Chen, G Zhang, F Sun, Optimal resource allocation for cognitive radio networks with primary user outage constraint. EURASIP J. Wireless Commun. Netw. **2015**(1), 239 (2015). doi:10.1186/s13638-015-0465-4

169. W-L Lin, C-H Lin, F-S Tseng, Performance analysis and power allocation strategy in single-antenna cognitive overlay systems. EURASIP J. Wireless Commun. Netw. **2015**(1), 249 (2015). doi:10.1186/s13638-015-0460-9

170. F Panahi, T Ohtsuki, Analytical modeling of cognitive heterogeneous cellular networks over Nakagami-m fading. EURASIP J. Wireless Commun. Netw. **2015**(1), 61 (2015). doi:10.1186/s13638-015-0277-6

171. M Sarijari, M Abdullah, G Janssen, A-J der Veen, On achieving network throughput demand in cognitive radio-based home area networks. EURASIP J. Wireless Commun. Netw. **2015**(1), 221 (2015). doi:10.1186/s13638-015-0448-5

172. I Suliman, J Lehtomaki, K Umebayashi, On the effect of false alarm rate on the performance of cognitive radio networks. EURASIP J. Wireless Commun. Netw. **2015**(1), 244 (2015). doi:10.1186/s13638-015-0474-3

173. Y Mehmood, C Gorg, M Muehleisen, A Timm-Giel, Mobile M2M communication architectures, upcoming challenges, applications, and future directions. EURASIP J. Wireless Commun. Netw. **2015**(1), 250 (2015). doi:10.1186/s13638-015-0479-y

174. Q Zhang, Z Feng, Y Zhang, T Yang, Hybrid frequency allocation scheme for capacity improvement in densely deployed small cells. EURASIP J.

Wireless Commun. Netw. **2015**(1), 152 (2015). doi:10.1186/s13638-015-0387-1

175. K Huang, JG Andrews, in *Global Telecommun. Conf. (GLOBECOM'11)*. A stochastic-geometry approach to coverage in cellular networks with multi-cell cooperation, (2011), pp. 1–5. doi:10.1109/GLOCOM.2011.6134295

176. F Baccelli, A Giovanidis, A stochastic geometry framework for analyzing pairwise-cooperative cellular networks. IEEE Trans. Wireless Commun. **14**(2), 794–808 (2015)

177. Ericsson Mobility Report (2015). http://www.ericsson.com/res/docs/2015/mobility-report/ericsson-mobility-report-nov-2015.pdf

178. HS Dhillon, JG Andrews, Downlink rate distribution in heterogeneous cellular networks under generalized cell selection. IEEE Wireless Commun. Lett. **3**(1), 42–45 (2014). doi:10.1109/WCL.2013.110713.130709

179. L Le, V Lau, E Jorswieck, N-D Dao, A Haghighat, D Kim, T Le-Ngoc, Enabling 5G mobile wireless technologies. EURASIP J. Wireless Commun. Netw. **2015**(1), 218 (2015). doi:10.1186/s13638-015-0452-9

180. T Bai, RW Heath, in *IEEE Int. Workshop Signal Processing Advances in Wireless Commun. (SPAWC)*. Asymptotic SINR for millimeter wave massive MIMO cellular networks, (2015), pp. 620–624. doi:10.1109/SPAWC.2015.7227112

181. T Bai, RW Heath, in *IEEE Global Conf. Signal and Information Processing (GlobalSIP)*. Asymptotic coverage and rate in massive MIMO networks, (2014), pp. 602–606. doi:10.1109/GlobalSIP.2014.7032188